Dalton Transactions

An international journal of inorganic chemistry

www.rsc.org/dalton

Volume 42 | Number 42 | 14 November 2013 | Pages 14929–15236

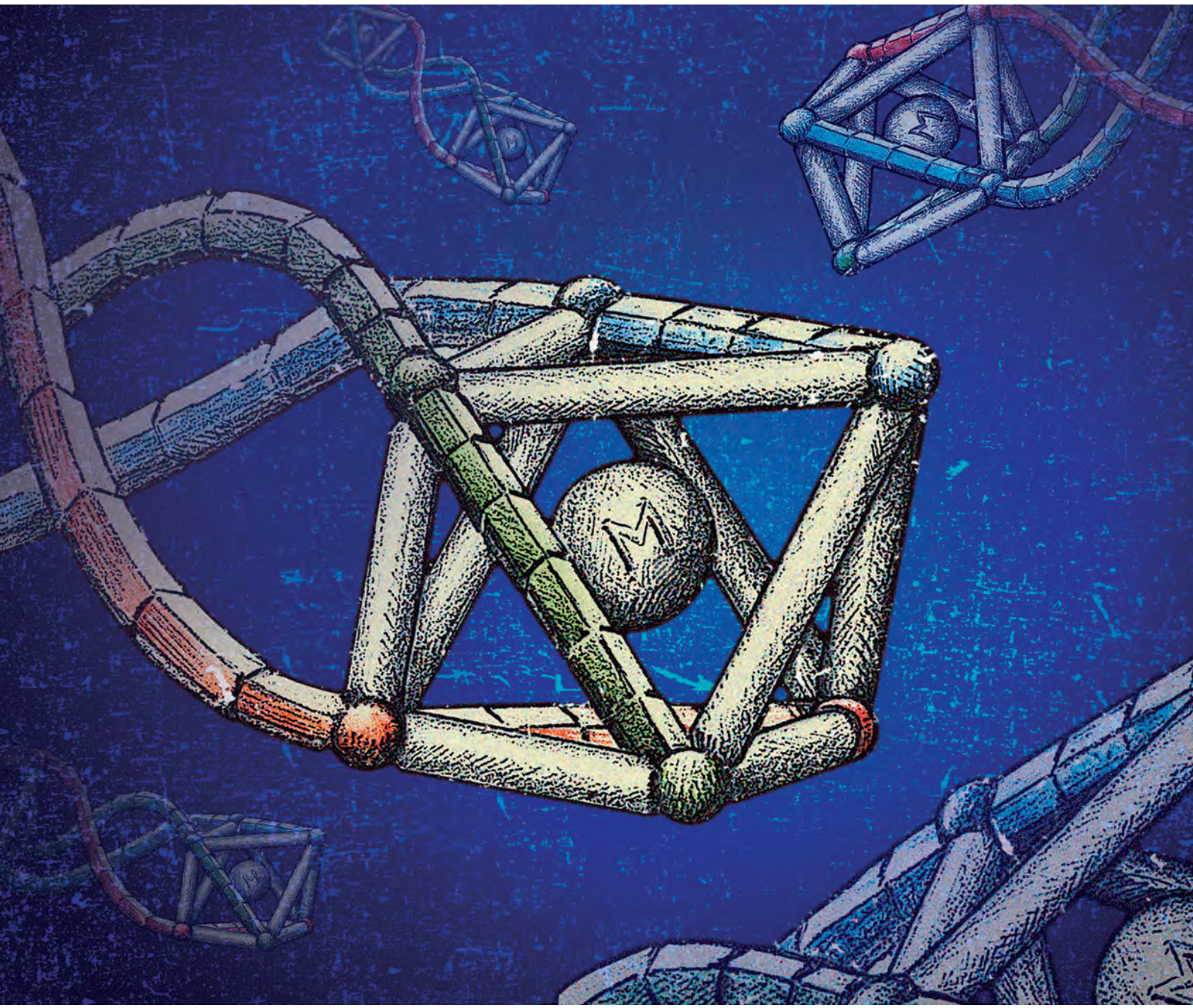

ISSN 1477-9226

RSC Publishing

COVER ARTICLE

Scott *et al.*

Optically pure heterobimetallic helicates from self-assembly and click strategies

1477-9226(2013)42:42;1-I

Dalton Transactions

RSC Publishing

PAPER

View Article Online
View Journal | View Issue

Open Access Article. Published on 01 August 2013. Downloaded on 10/17/2025 10:08:07 PM.
This article is licensed under a Creative Commons Attribution 3.0 Unported Licence.

Cite this: *Dalton Trans.*, 2013, **42**, 14967

Optically pure heterobimetallic helicates from self-assembly and click strategies†

Suzanne E. Howson, Guy J. Clarkson, Alan D. Faulkner, Rebecca A. Kaner, Michael J. Whitmore and Peter Scott*

Received 27th June 2013,
Accepted 31st July 2013

DOI: 10.1039/c3dt51725j

www.rsc.org/dalton

Single diastereomer, diamagnetic, octahedral Fe(II) tris chelate complexes are synthesised that contain three pendant pyridine proligands pre-organised for coordination to a second metal. They bind Cu(I) and Ag(I) with coordination geometry depending on the identity of the metal and the detail of the ligand structure, but for example homohelical (Δ_{Fe},Δ_{Cu}) configured systems with unusual trigonal planar Cu cations are formed exclusively in solution as shown by VT-NMR and supported by DFT calculations. Similar heterobimetallic tris(triazole) complexes are synthesised *via* clean CuAAC reactions at a tris-(alkynyl) complex, although here the configurations of the two metals differ (Δ_{Fe},Λ_{Cu}), leading to the first optically pure heterohelicates. A second series of Fe complexes perform less well in either strategy as a result of lack of preorganisation.

Introduction

Metallo-helicate chemistry is almost exclusively confined to D_n-symmetric systems (n = 2–4) self-assembled from symmetric ditopic ligands as shown in Fig. 1(a). Heterobimetallic helicates, although relatively rare, provide an opportunity to synthesise C_n or lower symmetry systems in which two different bidentate coordinating groups are connected *via* a linker, and using two metals which have a preference for one end of the ligand over the other[1–6] [Fig. 1(b)]. Alternatively, in a multi-step synthesis of heterobimetallics, one (inert) metal is coordinated before a second coordination site and metal are introduced.[7] With fully inert systems, enantiomers can sometimes be resolved using *e.g.* chromatography to isolate (highly) optically enriched helicates[2,7] but to our knowledge, the self-assembly of optically pure (or at least highly enantiomerically enriched) heterobimetallic complexes has not been reported. This could provide strategies for the synthesis of large complexes in which precise placement of functionality and charge can be achieved *i.e.* towards systems which mimic natural self-assembling systems such as protein α-helices.

We have recently shown that a range of single diastereomer diimine complexes of Fe(II) can be made very readily using 2-pyridinecarboxaldehyde and simple phenylethanamines as the source of chirality (Fig. 2).[8,9] The diastereomeric ratios were determined by ^{1}H NMR spectroscopy to be >200 : 1 in all cases and this unique system has since been exploited by ourselves[10] and others[11,12] to generate novel architectures. Since

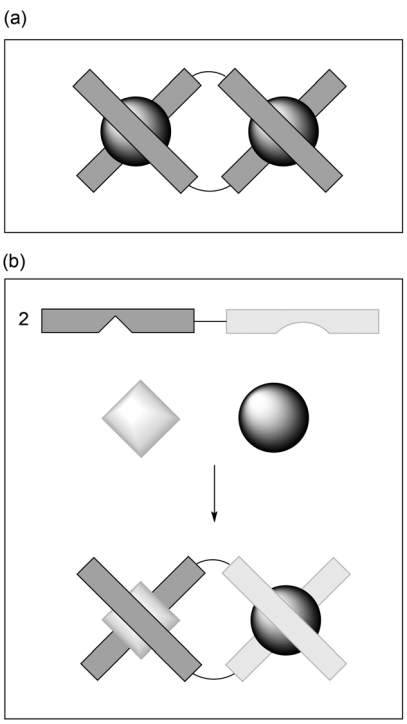

Fig. 1 Showing (a) a conventional D_2-symmetric helicate assembled from a bis-(bidentate) ligand and two metal ions; and (b) a heterobimetallic C_2-symmetric system.

Department of Chemistry, University of Warwick, Gibbet Hill Road, Coventry, CV4 7AL, UK. E-mail: peter.scott@warwick.ac.uk; Fax: +44 (0) 24 7657 2710; Tel: +44 (0) 24 7652 3238

†CCDC 947140–947142. For crystallographic data in CIF or other electronic format see DOI: 10.1039/c3dt51725j

Open Access Article. Published on 01 August 2013. Downloaded on 10/17/2025 10:08:07 PM.
This article is licensed under a Creative Commons Attribution 3.0 Unported Licence.

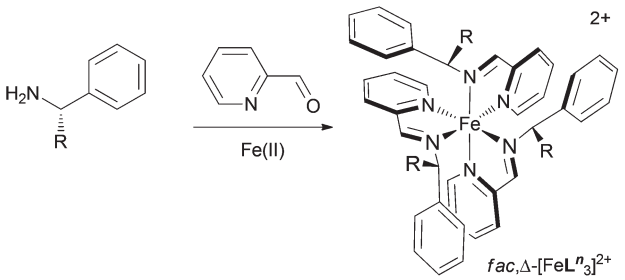

Fig. 2 The self-assembling diastereomerically pure tris-chelate system used in this work.[8,9]

these monometallic Fe(II) units are relatively inert, the opportunity arises to carry out further reactions as one might with say a ruthenium tris(chelate).[7]

In this report we describe the coordination of a second metal to either a preformed second coordination site or one created *in situ* by copper(I)-catalysed Huisgen 1,3-dipolar cycloaddition (CuAAC).

Results and discussion

In principle, suitable trifunctional metallo-ligands based on the complexes of Fig. 2 might be formed by functionalising at the phenylglycinol-derived site R or at the pyridine. We address these two approaches with ligands $\mathbf{L}^{1-6}$ and $\mathbf{L}^{7-10}$ respectively (Fig. 3).

Pyridinyl ethers $\mathbf{L}^{1-2}$

The use of three equivalents of 2-(pyridin-2-methoxy)-1-phenylethanamine in a one-pot synthesis with three equivalents of 2-pyridinecarboxaldehyde and one equivalent of $Fe(ClO_4)_2 \cdot 6H_2O$ led to the formation of a complex of the type shown in Fig. 2 *fac*,Δ_{Fe},R_C-[Fe$\mathbf{L}^1{}_3$]$(ClO_4)_2$ (for $\mathbf{L}^1$ see Fig. 3). This complex formed as a single diastereomer (d.r. > 200 : 1) as shown by NMR spectroscopy.[8,9] The complex *fac*,Δ_{Fe},R_C-[Fe$\mathbf{L}^2{}_3$]$(ClO_4)_2$ was synthesised in a similar manner.

An X-ray molecular structure of *fac*,Δ_{Fe},R_C-[Fe$\mathbf{L}^1{}_3$]$(ClO_4)_2$ was determined (Fig. 4). The Fe tris(diamine) unit is in the expected *fac* arrangement with three sets of π-stacks between phenyl and pyridine units.[8,9] The pendant pyridine substituents are arranged in a 3-fold symmetric array but with opposite helicity to the Fe unit. This is as we expected since the stereogenic centres at C(7) act as "corners" effectively switching the sense of twist. A similar phenomenon was displayed in a bimetallic structure based on this tris(diimine) unit.[10] It proved difficult with the X-ray data available to discriminate between the structure shown and an alternative with pyridine N atoms at the inward facing positions. Nevertheless we were encouraged that the system appeared to be preorganised to bind a second metal.

While a range of reactions of *fac*,Δ_{Fe},R_C-[Fe$\mathbf{L}^1{}_3$]$(ClO_4)_2$ and *fac*,Δ_{Fe},R_C-[Fe$\mathbf{L}^2{}_3$]$(ClO_4)_2$ with Fe(II), Co(II/III), and Zn(II) sources failed to give stable bimetallic species, the addition of CuI or $AgClO_4$ to acetonitrile solutions resulted in the formation of

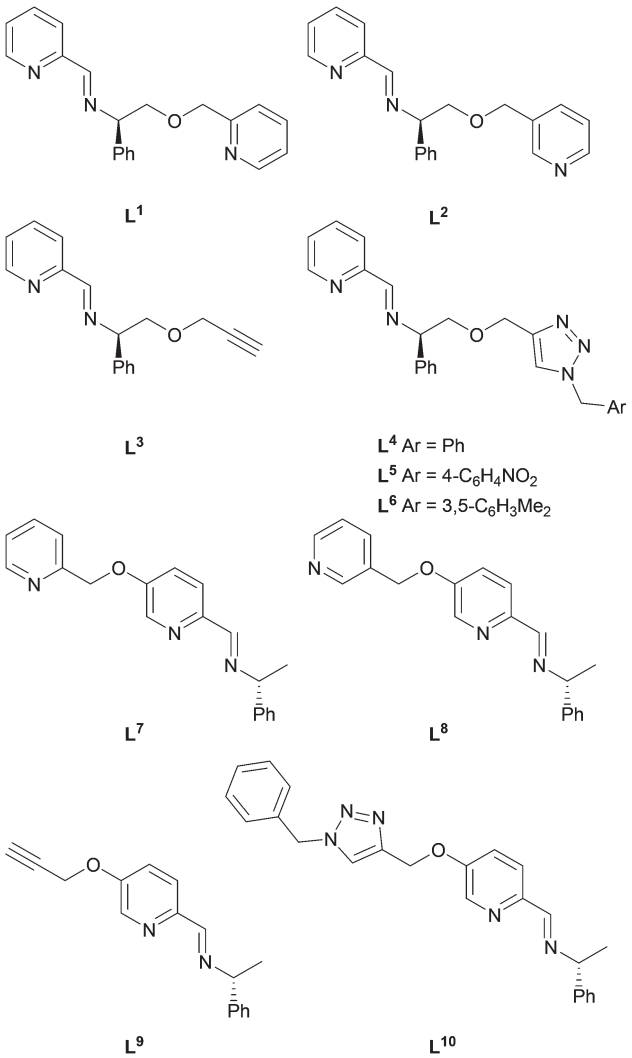

Fig. 3 Ligands $\mathbf{L}^1$–$\mathbf{L}^{10}$ assembled *in situ via* condensation or CuAAC reactions.

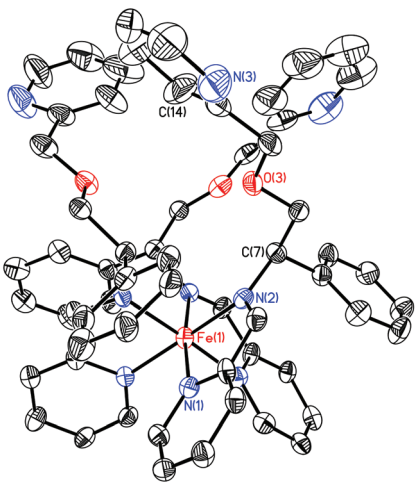

Fig. 4 Structure of the cation in the unit cell of *fac*,Δ_{Fe},R_C-[Fe$\mathbf{L}^1{}_3$]$(ClO_4)_2 \cdot$ 1.5(MeOH) (H atoms, counterions and solvent molecules omitted for clarity). Thermal ellipsoids are shown at 50% probability. Selected bond lengths (Å) and angles (°): Fe(1)–N(1) 1.963(4), Fe(1)–N(2) 1.986(4); N(1)–Fe(1)–N(2) 80.78(16).

 This journal is © The Royal Society of Chemistry 2013

Open Access Article. Published on 01 August 2013. Downloaded on 10/17/2025 10:08:07 PM.
This article is licensed under a Creative Commons Attribution 3.0 Unported Licence.

the four new crystalline heterobimetallic complexes Δ_{Fe},Δ_{Cu}, R_C-[Fe$\mathbf{L^1}_3$Cu](ClO$_4$)$_2$I, $\Delta_{Fe},\Delta_{Cu},R_C$-[Fe$\mathbf{L^2}_3$CuI](ClO$_4$)$_2$, Δ_{Fe},R_C-[Fe$\mathbf{L^1}_3$Ag(CH$_3$CN)](ClO$_4$)$_3$ and Δ_{Fe},R_C-[Fe$\mathbf{L^2}_3$Ag(CH$_3$CN)](ClO$_4$)$_3$; the absolute configurations are discussed later.

Coordination of the second metal led to characteristic changes in the ^{1}H NMR spectra. The starting material *fac*,Δ_{Fe}, R_C-[Fe$\mathbf{L^1}_3$](ClO$_4$)$_2$ [Fig. 5(a)] shows the two doublets separated by *ca.* 0.06 ppm for the CH$_2$ group between the ether oxygen and the pyridine ring while in the bimetallic complex Δ_{Fe},Δ_{Cu}, R_C-[Fe$\mathbf{L^1}_3$Cu](ClO$_4$)$_2$I this increases to *ca.* 0.20 ppm (b). These CH$_2$ protons are held in a more rigid conformation compared with the monometallic structure and this leads to a less complete averaging of the magnetic environments. The ^{1}H NMR spectrum of Δ_{Fe},R_C-[Fe$\mathbf{L^1}_3$Ag(CH$_3$CN)](ClO$_4$)$_3$ was similar. Low temperature (233 K) ^{1}H NMR spectra of the two complexes revealed no further changes suggesting that in both cases essentially one diastereomer is present in solution at level detectable by NMR spectroscopy. Microanalyses were consistent with the presence of the second metal and appropriate counter-ions. In the case of Δ_{Fe},R_C-[Fe$\mathbf{L^1}_3$Ag(CH$_3$CN)](ClO$_4$)$_3$, microanalysis was consistent with a single molecule of acetonitrile per complex, thus making up the expected tetrahedral geometry at the Ag(I) ion.

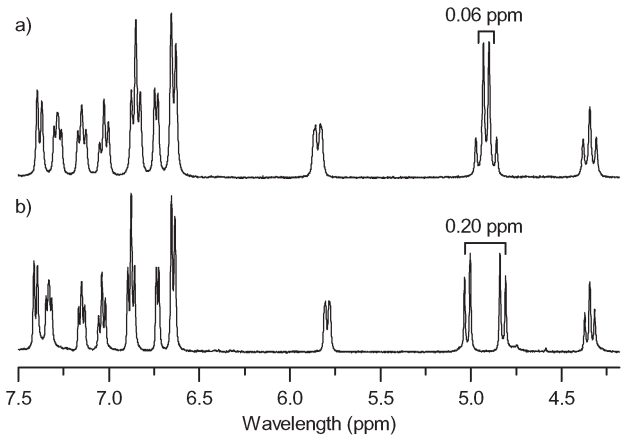

Fig. 5 ^{1}H NMR spectra in CD$_3$CN of (a) *fac*,Δ_{Fe},R_C-[Fe$\mathbf{L^1}_3$](ClO$_4$)$_2$ and (b) $\Delta_{Fe},\Delta_{Cu},R_C$-[Fe$\mathbf{L^1}_3$Cu](ClO$_4$)$_2$I.

In contrast to the $\mathbf{L^1}$ system, the ^{1}H NMR spectrum of $\Delta_{Fe},\Delta_{Cu},R_C$-[Fe$\mathbf{L^2}_3$CuI](ClO$_4$)$_2$ showed that the peaks relating to the protons close to the second binding site (*i.e.* OCH_2*Py*) were broadened. At lower temperatures these peaks were sharper (Fig. 6, peaks marked *) indicating that some exchange process is being slowed. This may be due to the presence of two diastereomers (Δ_{Fe},Δ_{Cu} and Δ_{Fe},Λ_{Cu}) or fluxionality at the Cu(I) binding site either associated with conformers or iodide substitution (see calculations later). We also observe in the VT

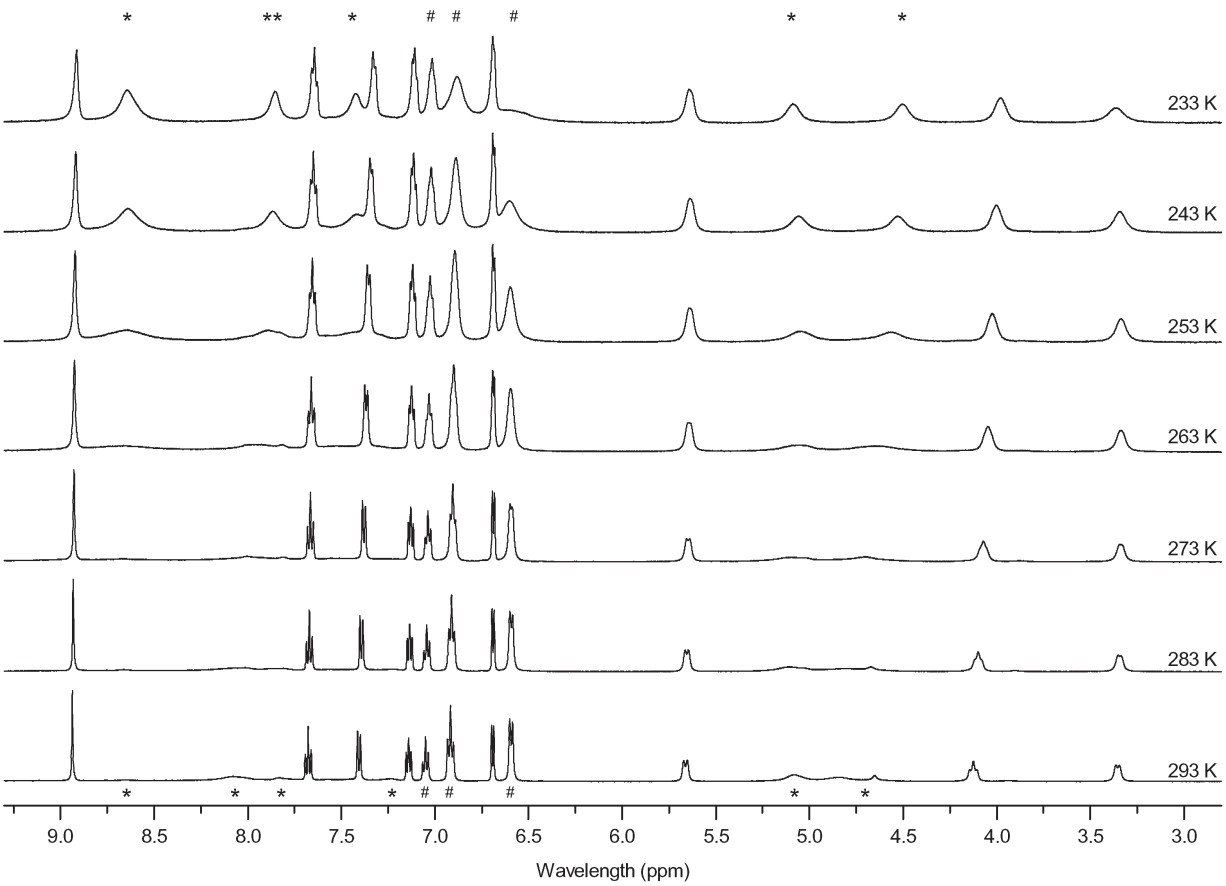

Fig. 6 VT ^{1}H NMR spectra of [Fe$\mathbf{L^2}_3$CuI](ClO$_4$)$_2$ in d_3-acetonitrile (* OCH_2*Py*, # *Ph*).

Open Access Article. Published on 01 August 2013. Downloaded on 10/17/2025 10:08:07 PM.
This article is licensed under a Creative Commons Attribution 3.0 Unported Licence.

Table 1 Energies and angles from DFT calculations of Δ_{Fe},R_C-[Fe$\mathbf{L^1}_3$Cu]$^{3+}$ and Δ_{Fe},R_C-[Fe$\mathbf{L^2}_3$CuI]$^{2+}$

Complex	Isomer	Energy (kcal mol^{-1})	Sum of angles about Cu (°)	Out of plane angle θ (°)[a]
[Fe$\mathbf{L^1}_3$Cu]$^{3+}$	$\Delta_{Fe}\Delta_{Cu}$	−19 512.10	352.45	9.22
(2-pyridinyl)	$\Delta_{Fe}\Lambda_{Cu}$	−19 508.07	356.57	6.19
[Fe$\mathbf{L^2}_3$CuI]$^{2+}$	$\Delta_{Fe}\Delta_{Cu}$	−19 655.23	315.01	23.63
(3-pyridinyl)	$\Delta_{Fe}\Lambda_{Cu}$	−19 652.19	312.19	24.45

[a] See Fig. 8.

^{1}H NMR spectra that the peaks corresponding to the phenyl rings (Fig. 6, peaks marked #) broaden as the temperature decreases with the extent of broadening *ortho* > *meta* > *para*. This is consistent with restricted CH–Ph bond rotations which cause averaging of the magnetic environments at room temperature.[13]

The ^{1}H NMR spectrum of Δ_{Fe},R_C-[Fe$\mathbf{L^2}_3$Ag(CH$_3$CN)](ClO$_4$)$_3$ is consistent with coordination of Ag(I); no broadening of signals associated with the second binding site was observed at accessible temperatures and only one diastereomer was observed.

Density functional theory (DFT) calculations using ADF2009 (version 2009.01)[14] were used to investigate the structures of the Fe–Cu bimetallic complexes with $\mathbf{L^1}$ and $\mathbf{L^2}$. In addition to the helicity at Fe which is essentially fixed, the pitch sense of the propeller arrangement of the pendant pyridine ligands about the Cu(I) centre needs also to be taken into account, and it was found that both homohelical $\Delta_{Fe}\Delta_{Cu}$ and heterohelical $\Delta_{Fe}\Lambda_{Cu}$ isomers for both the 2- and 3-pyridinyl complexes could be optimised (Table 1). In both cases the input geometries around Cu(I) were based on the related X-ray structure of [Cu(3-methylpyridine)$_3$I] which has a distorted tetrahedral geometry.[15]

For the 2-pyridinyl ($\mathbf{L^1}$) complex, as the optimisations progressed the Cu–I bond was broken in both enantiomers, resulting in approximately trigonal planar geometries. As a result, the iodide anion was deleted from these calculations to allow convergence. The calculations reveal that the homohelical $\Delta_{Fe}\Delta_{Cu}$ isomer is lower in energy by *ca.* 4 kcal mol^{-1} compared to the heterohelical $\Delta_{Fe}\Lambda_{Cu}$ isomer. Fig. 7 shows that the $\Delta_{Fe}\Delta_{Cu}$ isomer in (a) is more longitudinally extended than $\Delta_{Fe}\Lambda_{Cu}$ (b) as further indicated by the Fe–Cu distances (*ca.* 6.15 Å *vs.* 6.44 Å) and this is accompanied by; (i) reduction of unfavourable steric interactions between the pyridinyl ethers and the phenyl groups on the neighbouring ligands; and (ii) an increase in the magnitude of the propeller pitch‡ of the (Py)$_3$Cu units from *ca.* 36° to 49°. Whatever the origins of the energy difference – there are undoubtedly a number of competing factors – the calculations suggest the $\Delta_{Fe}\Delta_{Cu}$ isomer will be formed exclusively, at least at the level that can be determined by NMR spectroscopy, and indeed this is consistent with observations.

‡The propeller pitch is defined as the angle between mean plane of the three pyridine N atoms and that of a pyridine ligand.

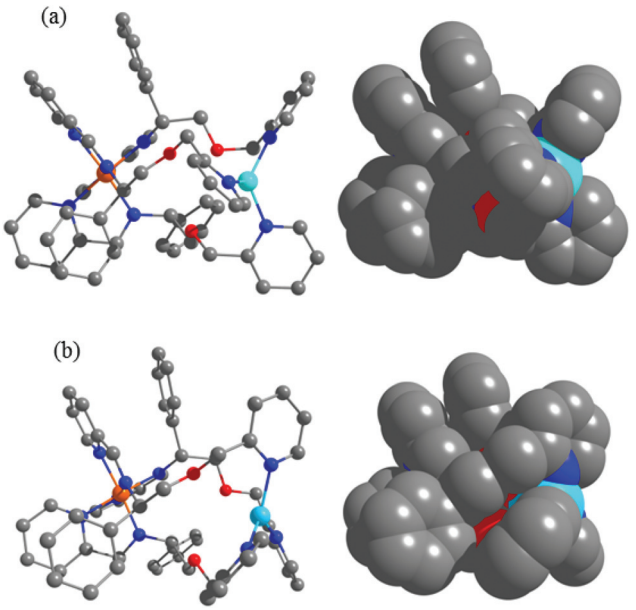

Fig. 7 Optimised structures and space-fill representations of (a) $\Delta_{Fe}\Delta_{Cu},R_C$-[Fe$\mathbf{L^1}_3$Cu]$^{3+}$ where the propeller pitch of the pyridine units at the planar Cu(I) centre (blue) is most pronounced; and (b) $\Delta_{Fe}\Lambda_{Cu},R_C$-[Fe$\mathbf{L^1}_3$Cu]$^{3+}$.

We were interested to investigate further the unusual[16] preference for trigonal planar Cu(I) geometry, specifically if this is a result of inherent chelate constraints in the ligand system [Fe$\mathbf{L^1}_3$]$^{2+}$ or from steric effects arising from 2-substitution of the pyridine. For these purposes we studied the model monometallic systems [Cu(2-methylpyridine)$_3$I] and [Cu(3-methylpyridine)$_3$I]. For both isomers, structures were optimised with a range of fixed Cu···I distances. The results in Fig. 8 show that for the 2-methylpyridine complex (filled squares) the energy *decreases* as the iodide ligand dissociates and the Cu(I) approaches the trigonal planar arrangement (*i.e.* as the out of plane angle $\theta \rightarrow 0°$). In contrast, the 3-methylpyridine system

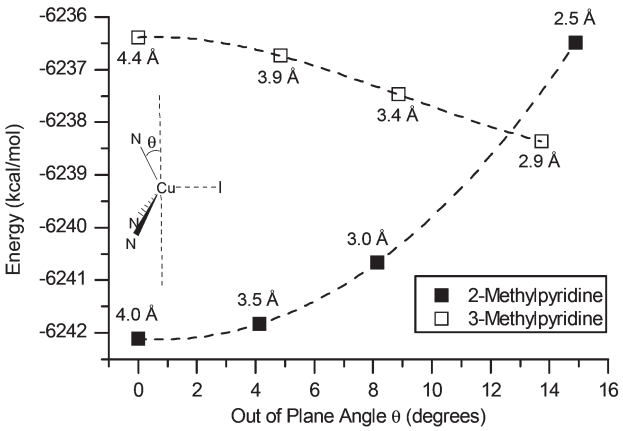

Fig. 8 Optimised energies *versus* out of plane angle θ for [Cu(methylpyridine)$_3$I] isomers on linear elongation of the Cu···I vector. Cu–I distances indicated at each point.

This journal is © The Royal Society of Chemistry 2013

Open Access Article. Published on 01 August 2013. Downloaded on 10/17/2025 10:08:07 PM.
This article is licensed under a Creative Commons Attribution 3.0 Unported Licence.

(open squares) *increases* in energy as the iodide dissociates, albeit more gradually, and indeed a tetrahedral structure is observed for [Cu(3-methylpyridine)$_3$I] by X-ray crystallography.[15] It would appear then that the preference for trigonal planar geometry about Cu(I) in the $\mathbf{L^1}$ system is expected from a steric effect of the 2-substitution alone, notwithstanding any influence of conformational strain.

Consistent with the observed and calculated structure of [Cu(3-methylpyridine)$_3$I], DFT calculations on $[\mathrm{Fe}\mathbf{L^2}_3\mathrm{CuI}]^{2+}$ isomers subsequently predicted tetrahedral geometries around Cu(I) in both $\Delta_{Fe}\Delta_{Cu}$ and $\Delta_{Fe}\Lambda_{Cu}$ isomers, with the homohelical isomer being the more stable (*ca.* 3 kcal mol^{-1}).

The electronic spectra of these $\mathbf{L^1}$ and $\mathbf{L^2}$ systems have some unusual features. UV-Vis absorbance spectra shown in Fig. 9 show familiar strong bands in the region 220–320 nm, corresponding to π–π* transitions within the ligands, three further peaks corresponding to MLCT bands are observed at 380, 520 and 540 nm respectively. In both cases, Cu(I) coordination results in an increase in intensity of π–π* region of the spectra, a decrease in the intensity of the MLCT bands between 460–650 nm and an increase at 360 nm. These Fe(II) based CT transitions are likely to be strongly affected by structural changes at the metal, but no such perturbation is evident from crystallography or calculations. We suggest that the presence of the nearby cationic charge of the Cu(I) is responsible for this change in relative intensity. For the π–π* region the change may be a result of ordering by coordination of the heterocycles to Cu(I). In the corresponding CD spectra measured on the same cuvette (Fig. 10) the picture is of a general reduction in intensity for reasons unknown, but evidently from the UV spectra this is not an error from concentration measurement.

Click reactions of $\mathbf{L^3}$ alkynyl complex; complexes $\mathbf{L^{4-6}}$

Interestingly, despite the popularity of the CuAAC reaction in synthetic, biological and materials chemistry, relatively few examples have been reported on pre-formed metal complexes. The majority of these are found in the synthesis of rotaxanes and catenanes where a metal is used to template components ("*gathering and threading*").[17–25] Other examples exist for inert complex systems.[26–32] In other cases [Zn(II), Mn(II), Fe(III), Co(II)] click reactions do not proceed cleanly; the metals are easily displaced by the Cu 'click' catalyst, either directly or *via* electron transfer.[28]

The diastereomerically pure compound *fac*,Δ_{Fe},R_C-$[\mathrm{Fe}\mathbf{L^3}_3]$-$(\mathrm{ClO_4})_2$ (for $\mathbf{L^3}$ see Fig. 3) was synthesised using the standard

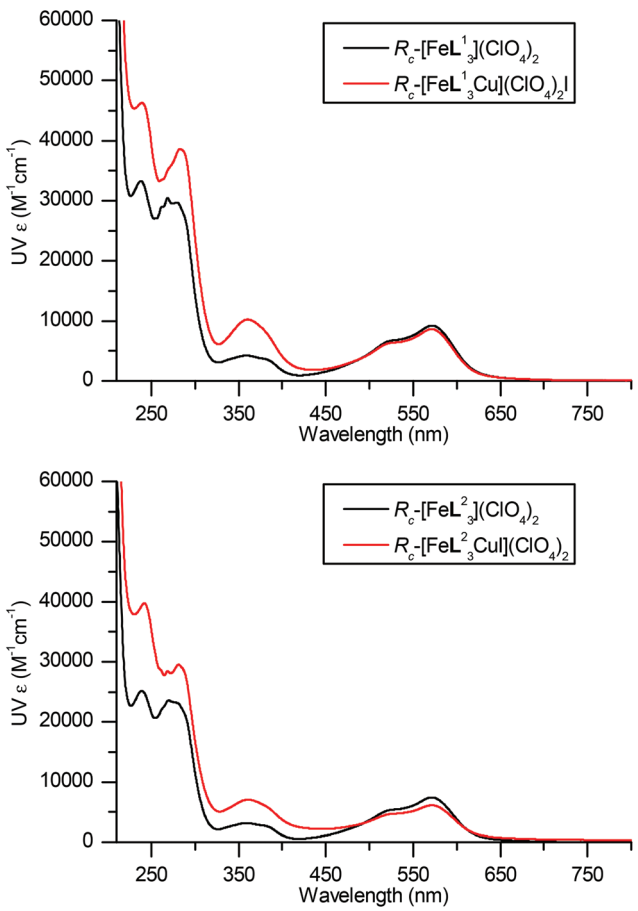

Fig. 9 UV/vis spectra of Fe and Fe/Cu complexes of $\mathbf{L^1}_3$ and $\mathbf{L^2}$. Path length 1.0 cm and concentration 3.3 mM.

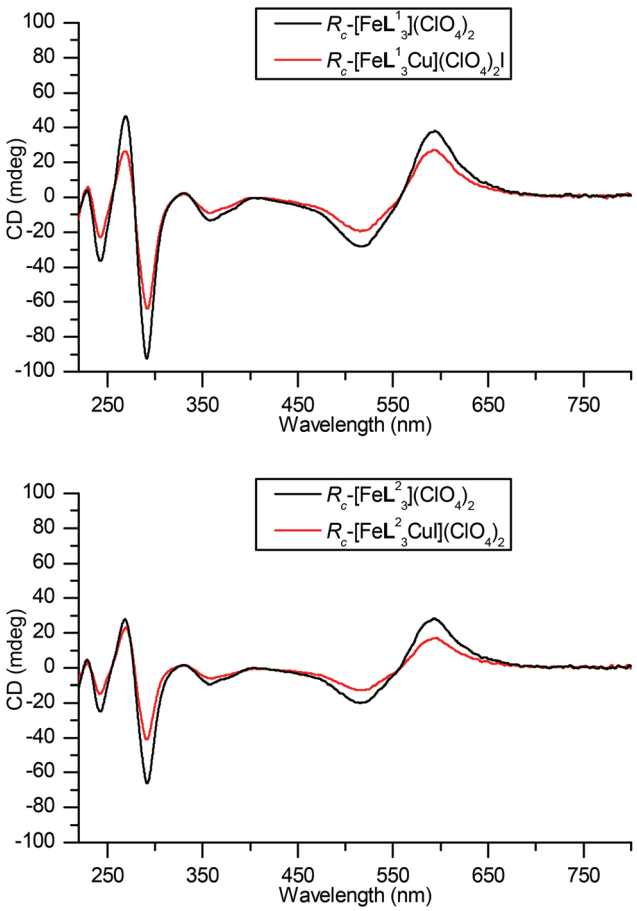

Fig. 10 CD spectra of Fe and Fe/Cu complexes of $\mathbf{L^1}_3$ and $\mathbf{L^2}$. Path length 1.0 cm and concentration 3.3 mM.

Open Access Article. Published on 01 August 2013. Downloaded on 10/17/2025 10:08:07 PM.
This article is licensed under a Creative Commons Attribution 3.0 Unported Licence.

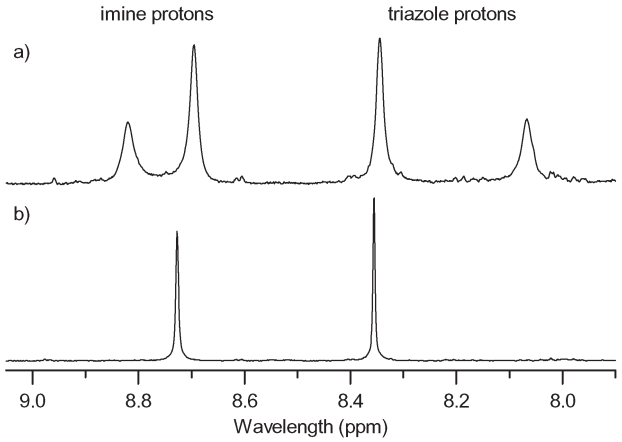

Fig. 11 Imine/triazole region in the ^{1}H NMR spectra in CD_3CN at 233 K for the 'click' reactions between *fac*,Δ_{Fe},R_C-[Fe$\mathbf{L^3}_3$]$(ClO_4)_2$ and BnN_3 with (a) 0.3 eq. CuI and (b) 1.0 eq. CuI.

one-pot synthesis with the propargylic ether derivative of (*R*)-2-phenylglycinol. This complex is of particular interest due to its potential to undergo copper(I)-catalysed Huisgen 1,3-dipolar cycloaddition (CuAAC) 'click' reactions between the three alkyne units and organic azides. Accordingly it was treated with benzyl azide in the presence of dry triethylamine and a catalytic amount of copper(I) iodide (0.3 eq. per complex) in dry acetonitrile to give a purple solid. The ^{1}H NMR spectrum at ambient temperature contained only one set of ligand resonances, however at low temperature (233 K), the ^{1}H NMR spectrum revealed that there were in fact two species present in the recrystallised sample in the ratio 1 : 1.7 [Fig. 11(a)]. The reaction was repeated using a stoichiometric amount of copper(I) iodide (1.0 equivalent per Fe). The resulting low temperature ^{1}H NMR spectrum showed only one set of peaks [Fig. 11(b)] and microanalysis indicated that copper(I) iodide was present in a 1 : 1 ratio with the complex. Hence, the spectrum shown in Fig. 11(a) arises from an equilibrium between two complexes *fac*,Δ_{Fe},R_C-[Fe$\mathbf{L^4}_3$]$^{2+}$ and Δ_{Fe},R_C-[Fe$\mathbf{L^4}_3$Cu]$^{3+}$ as shown in Scheme 1.

Slow vapour diffusion of ethyl acetate into an acetonitrile solution of Δ_{Fe},R_C-[Fe$\mathbf{L^4}_3$Cu]$(ClO_4)_2$I in air resulted in the formation of single crystals that were suitable for X-ray diffraction. The solid state structure is shown in Fig. 12 along with key bond lengths and angles. The asymmetric unit contains one complex and a mixture of perchlorate and triiodide (resulting from oxidation of iodide in air) as the counterions. The Fe(II) and Cu(I) cations lie on a threefold axis. The complex has an approximately octahedral arrangement around Fe(II) and a trigonal planar arrangement around Cu(I), with a distance between the metal centres of *ca.* 6.14 Å. Most interestingly, the sense of the helicity at the Cu(I) centre is opposite to that at the Fe(II) centre (*i.e.* Δ_{Fe},Λ_{Cu}). Nevertheless this is not a *meso-cate* since the metals are different and thus the system is chiral. Hence, we would describe this as the first example of an optically pure heterohelicate.[33]

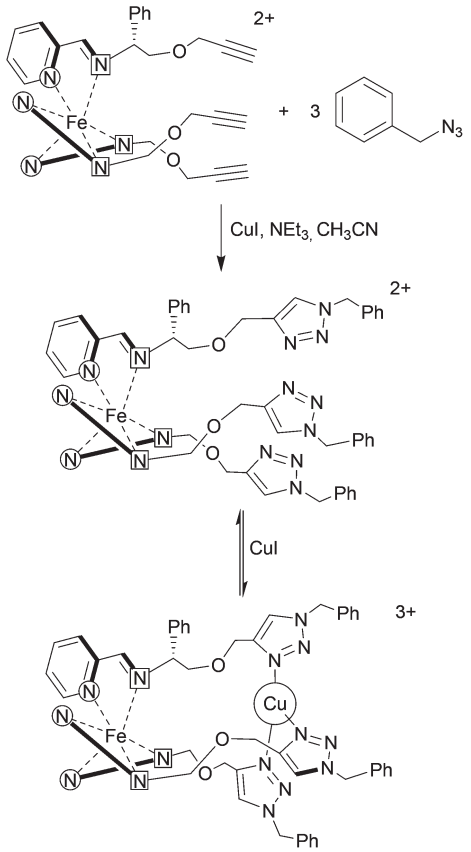

Scheme 1 'Click' reaction between *fac*,Δ_{Fe},R_C-[Fe$\mathbf{L^3}_3$]$(ClO_4)_2$ and BnN_3 resulting in an equilibrium between *fac*,Δ_{Fe},R_C-[Fe$\mathbf{L^4}_3$]$^{2+}$ and Δ_{Fe},R_C-[Fe$\mathbf{L^4}_3$Cu]$^{3+}$.

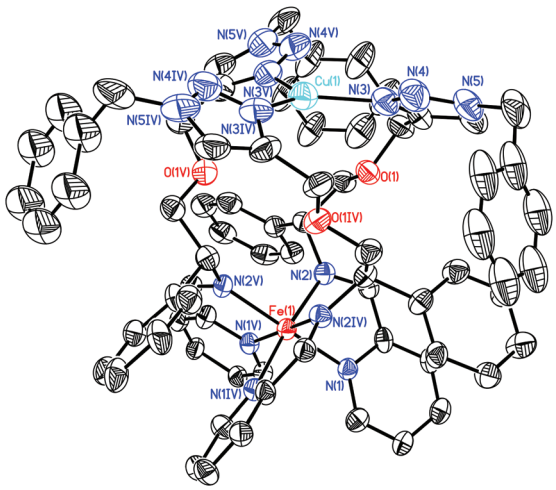

Fig. 12 Structure of the cation in the asymmetric unit of Δ_{Fe},Λ_{Cu},R_C-[FeCu$\mathbf{L^4}_3$]$(ClO_4)_{2.66}(I_3)_{0.33}$ (H atoms and counterions omitted for clarity). Thermal ellipsoids are shown at 30% probability. Selected bond lengths (Å) and angles (°): Fe(1)–N(1) 1.958(4), Fe(1)–N(2) 1.982(5), Cu(1)–N(3) 2.002(8); N(1)–Fe(1)–N(2) 81.46(19), N(3)#2–Cu(1)–N(3) 119.982(10).

In addition to the usual[8,9] three sets of inter-ligand parallel-offset π-stacking interactions in the Fe unit there are three sets of CH–π interactions[34,35] present between the triazole benzyl

 This journal is © The Royal Society of Chemistry 2013

Open Access Article. Published on 01 August 2013. Downloaded on 10/17/2025 10:08:07 PM.
This article is licensed under a Creative Commons Attribution 3.0 Unported Licence.

Table 2 Energies and angles from DFT calculations of Δ_{Fe},R_C-[Fe$\mathbf{L^4}_3$Cu]$^{3+}$

Δ_{Fe},R_C-[Fe$\mathbf{L^4}_3$Cu]$^{3+}$ diastereomer	Rotamer type[a]	Energy (kcal mol^{-1})	Relative energy (kcal mol^{-1})	Sum of angles about Cu(1) (°)
Heterohelical	A	−24 144.94	0	360.01
(Δ_{Fe},Λ_{Cu})	B	−24 145.35	+0.41	359.96
Homohelical	A	−24 132.48	+12.46	359.99
(Δ_{Fe},Δ_{Cu})	B	−24 135.67	+9.27	359.97

[a] Type A is as shown in Fig. 10 whereas in type B a rotation of *ca.* 180° about the N–C bond in the benzyl groups was made before optimisation *i.e.* benzyl groups point "up".

substituent and the CHCH_2O group on a neighbouring ligand. The Cu(I) is coordinated to the triazole rings *via* the 3-position *i.e.* the N(3) nitrogen atom, as expected on the basis of its higher basicity and perhaps also here a more favourable chelate conformation. There is nevertheless also some precedent for the coordination of metals to the 2-position [*i.e.* N(4)] in 1-substituted-1,2,3-triazole rings.[36]

The geometries of the homohelical $\Delta_{Fe}\Delta_{Cu}$ and heterohelical $\Delta_{Fe}\Lambda_{Cu}$ isomers of Δ_{Fe},R_C-[Fe$\mathbf{L^4}_3$Cu]$^{3+}$ were optimised and their energies calculated (Table 2) from density functional calculations as above. While the benzyl substituents on the triazole rings point down towards Fe(II) in the X-ray structure, various rotamers were also considered and optimised. The observed heterohelical isomer was found to be the lower in energy than the homohelical diastereomer by at least 9.27 kcal mol^{-1} such that we expect this structure exist exclusively in solution at equilibrium. Low temperature NMR studies are in agreement and on the basis of these calculations and the X-ray structure we can assign the solution species as heterohelical $\Delta_{Fe},\Lambda_{Cu},R_C$-[Fe$\mathbf{L^4}_3$Cu]$^{3+}$.

The origins of this stereoselection are not obvious, and indeed the sums of angles around Cu in the structures are all very close to 360° indicating a lack of strain here. While as for $\Delta_{Fe},\Delta_{Cu},R_C$-[Fe$\mathbf{L^1}_3$Cu]$^{3+}$ there are likely to be a number of contributing factors, examination of space-filling models reveals an absence here of steric compression between the triazole and the ether units in the neighbouring ligands, thus allowing the system to adopt the more favourable conformations in the linker chain of the heterohelical system.

Further examples of heterohelical bimetallic complexes with $\mathbf{L^5}$ and $\mathbf{L^6}$ (Fig. 3) were synthesised from click reactions between *fac*,Δ_{Fe},R_C-[Fe$\mathbf{L^3}_3$](ClO$_4$)$_2$ and the appropriate organic azides (3,5-dimethylbenzyl azide and 4-nitrobenzyl azide) in the presence of 1 equivalent of CuI per complex. In all cases, low temperature ^{1}H NMR spectra show only a single set of peaks consistent with a single diastereomer in solution.

The ability to remove Cu(I) from these bimetallic complexes would be attractive so a number of methods were attempted to remove Cu(I) post-'click' reaction. The use of a copper scavenger, *e.g.* Smopex-111, Smopex 112, CupriSorb™, EDTA or sodium sulfide, either removed no copper or caused complete decomposition of the complex by removing both Cu(I) and Fe(II). As an alternative was also attempted the ruthenium(II) catalysed 'click' reactions[37–39] but no reaction occurred. Conversely, the use of copper wire and PMDETA[40,41] as the catalyst caused complete decomposition. These results led us to consider the scope for functionalisation from the pyridine side of the monometallic complex.

Pyridinyl ethers $\mathbf{L^{7-8}}$

In order to compare the coordination behaviour above with that of pendant units attached to the pyridine ligands in the tris(chelate)Fe(II), the ligands $\mathbf{L^{7-8}}$ (Fig. 3) were designed. Subsequently, the use of 5-(2-pyridinyloxy)picolinaldehyde in the standard one-pot synthesis with (*R*)-α-methylbenzylamine and Fe(ClO$_4$)$_2$·6H$_2$O led to the formation of diastereomerically pure *fac*,Λ_{Fe},R_C-[Fe$\mathbf{L^7}_3$](ClO$_4$)$_2$ (d.r. > 200 : 1). The X-ray molecular structure (Fig. 13) shows in contrast to that in Fig. 4 that the three pyridinyl ether groups are not preorganised for binding a second metal, but is otherwise conventional.

Addition of 1 equivalent of CuI to an acetonitrile solution containing *fac*,Λ_{Fe},R_C-[Fe$\mathbf{L^7}_3$](ClO$_4$)$_2$·CH$_3$CN led to no significant changes in chemical shifts, suggesting that coordination of Cu(I) to the second binding site is weak in solution. The same observation was made on addition of AgClO$_4$. In further support of this, crystallisation of *fac*,Λ_{Fe},R_C-[Fe$\mathbf{L^7}_3$](ClO$_4$)$_2$ in the presence of AgClO$_4$ resulted in a partially refined X-ray molecular structure showing an extended lattice structure with each tris(chelate)Fe(II) unit coordinated to three different silver(I) units; the formation of this structure is presumably driven by lattice enthalpy.

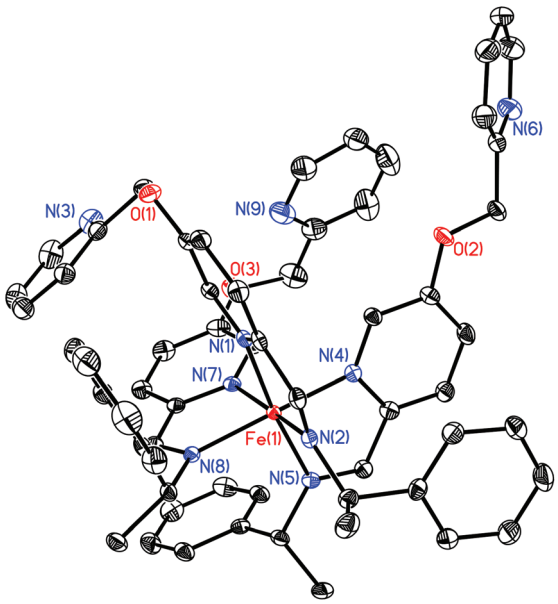

Fig. 13 Structure of the cation in the asymmetric unit of *fac*,Λ_{Fe},R_C-[Fe$\mathbf{L^7}_3$](ClO$_4$)$_2$·CH$_3$CN (H atoms, counterions and solvent molecules omitted for clarity). Thermal ellipsoids are shown at 50% probability. Selected bond lengths (Å) and angles (°): Fe(1)–N(1) 1.9745(14), Fe(1)–N(4) 1.9804(15), Fe(1)–N(7) 1.9748(15), Fe(1)–N(2) 1.9788(15), Fe(1)–N(5) 1.9789(15), Fe(1)–N(8) 1.9874(14); N(1)–Fe(1)–N(2) 81.58(6), N(4)–Fe(1)–N(5) 81.16(6), N(7)–Fe(1)–N(8) 81.22(6).

Open Access Article. Published on 01 August 2013. Downloaded on 10/17/2025 10:08:07 PM.
This article is licensed under a Creative Commons Attribution 3.0 Unported Licence.

In contrast to the $\mathbf{L^7}$ case above, reaction of three equivalents of both 5-(3-pyridinyloxy)picolinaldehyde and (*R*)-α-methylbenzylamine with $Fe(ClO_4)_2{\cdot}6H_2O$ gave a sample with broad NMR resonances. In solution the product slowly converted from purple to a paramagnetic red system on standing. This is likely to be due to the formation of a bis complex $[Fe\mathbf{L^8}_2]^{2+}$ as a result of the chelate effect; this 3-pyridinyl ligand is appropriately structured to coordinate in a tridentate fashion, as we have observed previously for a *tert*-leucinol derivative.[8]

Click reactions of $\mathbf{L^9}$ alkynyl complex; complexes of $\mathbf{L^{10}}$

The diastereomerically pure compound *fac*,Λ_{Fe},R_C-$[Fe\mathbf{L^9}_3](ClO_4)_2$ (for $\mathbf{L^9}$ see Fig. 3) was synthesised from the propargylic ether derivative of 5-hydroxy-2-picolinaldehyde. Copper(I)-catalysed Huisgen 1,3-dipolar cycloaddition (CuAAC) 'click' reactions between this complex and benzyl azide did not behave in the same way as for *fac*,Δ_{Fe},R_C-$[Fe\mathbf{L^3}_3](ClO_4)_2$ and the reaction with sub-stoichiometric (catalytic) amounts of CuI led to mixtures of starting material $[Fe\mathbf{L^9}_3](ClO_4)_2$ with $[Fe\mathbf{L^9}_2\mathbf{L^{10}}](ClO_4)_2$, $[Fe\mathbf{L^9}\mathbf{L^{10}}_2](ClO_4)_2$ and $[Fe\mathbf{L^{10}}_3](ClO_4)_2$ (Fig. 3) according to ^{1}H NMR spectroscopy (see ESI†) and mass spectrometry. With one equivalent of CuI per Fe centre (*i.e.* the conditions that cleanly gave Δ_{Fe},R_C-$[Fe\mathbf{L^4}_3Cu](ClO_4)_2I$) the majority product was $[Fe\mathbf{L^{10}}_3](ClO_4)_2$ but the without Cu^+ coordination. Addition of three equivalents of CuI per Fe unit or more, essentially complete click conversion was apparent, and the chemical shift difference for the diastereotopic O–CH_2–triazole group had widened to *ca.* 0.25 ppm indicating Cu^+ coordination *i.e.* $[Fe\mathbf{L^{10}}_3Cu]^{3+}$. Attempts to recrystallize this species for analysis led to slow decomposition and formation of red paramagnetic products. Presumably it suffers the same fate as the $\mathbf{L^8}$ system above, and for the same reasons.

Conclusion

Optically pure (highly enantiomerically enriched) heterobimetallic Fe–Cu and Fe–Ag helicates can be synthesised *via* the pre-formed monometallic Fe(II) complexes of $\mathbf{L^1}$ and $\mathbf{L^2}$. In both cases only a single isomer was observed by ^{1}H NMR spectroscopy and corresponding DFT calculations predict the ΔΔ homochiral isomer will form exclusively. Interestingly, formation of the trigonal planar geometry at Cu(I) is driven by the substitution pattern of the pyridine ligand, independently of any conformational effects in the bimetallic structure.

CuAAC 'click' reactions are most efficient on the monometallic complex of $\mathbf{L^3}$ and give Fe–Cu helicates directly. Again, a single isomer is formed but in this case both X-ray crystallography and DFT calculations support the exclusive formation of the $\Delta_{Fe}\Lambda_{Cu}$ heterochiral isomers. These compounds are the first examples of what might be called heterohelicates since they have opposite configurations at the metal but are not mesocates. Similar reactions on the Fe(II) complex of $\mathbf{L^9}$ are much less efficient presumably because the system, as demonstrated in the analogous pyridine series, is not preorganised for coordination of the Cu(I) ion; binding of the Cu(I) catalyst to the three triazoles appears to promote the reaction.

We are thus now in a position to confidently predict stereochemical properties in such bimetallic systems and will now move towards the synthesis of heterobimetallics designed for aqueous solubility.[33]

Experimental

General considerations

(*R*)-2-Phenylglycinol and 5-(hydroxy)picolinaldehyde were synthesised as previously described.[9,42,43] Deuterated solvents were purchased from Sigma-Aldrich and Cambridge Isotope Laboratories. Sodium hydride dispersions in mineral oil were placed in a Schlenk vessel under an inert atmosphere and washed three times with diethyl ether to remove the oil. The sodium hydride powder was then dried and stored in the dry box. Suitable precautions should be taken in the synthesis of organic azides.[44]

Where appropriate, reactions were carried out under argon using a dual manifold argon/vacuum line and standard Schlenk techniques or MBraun dry box. THF was pre-dried over sodium wire and then heated to reflux for 3 d under dinitrogen over potassium and degassed before use. Dried THF was stored in a glass ampoule under argon. All glassware and cannulae were stored in an oven at >375 K.

NMR spectra were recorded on Bruker Spectrospin 300/400/500 MHz spectrometers. Routine NMR assignments were confirmed by ^{1}H–^{1}H (COSY) and ^{13}C–^{1}H (HMQC) correlation experiments where necessary. The spectra were internally referenced using the residual protio solvent ($CDCl_3$, CD_3CN *etc.*) resonance relative to tetramethylsilane (δ = 0 ppm). ESI mass spectra were recorded on Bruker Esquire 2000 and Bruker MicroTOF spectrometers. Infra-Red spectra were measured using a Perkin-Elmer FTIR spectrometer. Elemental analyses were performed by Warwick Analytical Services, Coventry, UK and MEDAC Ltd, Surrey, UK.

The crystal data for Δ_{Fe},Λ_{Cu},R_C-$[Fe\mathbf{L^4}_3Cu](ClO_4)_2I$ (CCDC 947140) and *fac*,Λ_{Fe},R_C-$[Fe\mathbf{L^7}_3](ClO_4)_2$ (CCDC 947142) were collected using an Xcalibur Gemini diffractometer with a Ruby CCD area detector using CuK_α (λ = 1.54184 Å) radiation source. The crystal data for *fac*,Δ_{Fe},R_C-$[Fe\mathbf{L^1}_3](ClO_4)_2$ (CCDC 947141) was recorded by the National Crystallographic Service.[45] The structures were solved with the XS structure solution program using Direct Methods and refined with the ShelXL[46] refinement package using Least Squares minimisation.

Optical rotation measurements were performed on a Perkin Elmer Polarimeter 341 by Warwick Analytical Services, Coventry, UK. In all cases the following parameters were used: solvent methanol, temperature 20 °C, path length 100 mm, wavelength 589 nm.

Density functional optimisations were carried out using the Amsterdam Density Functional program (version 2009.01).[14] Starting points for geometry optimisations were taken from crystallographic data where available, and where unavailable,

 This journal is © The Royal Society of Chemistry 2013

Open Access Article. Published on 01 August 2013. Downloaded on 10/17/2025 10:08:07 PM. This article is licensed under a Creative Commons Attribution 3.0 Unported Licence.

starting structures were created from existing crystallographic fragments. Solution structures were optimised relative to acetonitrile (*vide infra*) using a triple-ζ plus polarisation basis set (TZP) on all atoms with the OPBE functional and Grimme's empirical correction for dispersion.[47] Small frozen cores[48] were used throughout. Calculations used integration level 5 (as defined by ADF) with convergence criteria of e = 0.0001 a.u., rad = 0.005 Å and grad = 0.001 a.u. $Å^{-1}$ for the total binding energy, Cartesian displacement and energy gradient respectively. Acetonitrile solvent effects were included based on the conductor-like screening model (COSMO) implemented in ADF.[49] Non-bonded radii used were H = 1.350 Å, C = 1.700 Å, N = 1.608 Å, Fe = 1.858 Å. A dielectric constant of 37.5 (acetonitrile) and an outer cavity radius of 2.76 Å were further used to parameterise the COSMO solvation cavity.

Synthesis

(*R*)-2-(Pyridin-2-methoxy)-1-phenylethanamine. 2-(Bromomethyl)-pyridine hydrobromide (3.50 g, 13.9 mmol, 0.95 eq.) was added as a solid to a stirred suspension of sodium hydride (0.43 g, 18.0 mmol, 1.3 eq.) in dry THF (20 ml). The solution was stirred for 30 min at ambient temperature and then heated to 55 °C for 45 min, all under partial vacuum. (*R*)-2-Phenylglycinol (2.00 g, 14.6 mmol) was dissolved in dry THF (10 ml) and was added dropwise to a stirred suspension of sodium hydride (0.70 g, 29.2 mmol, 2.0 eq.) in dry THF (20 ml). This solution was stirred for 1 h at ambient temperature under partial vacuum. The (*R*)-2-phenylglycinol–NaH solution was added to the 2-(bromomethyl)-pyridine hydrobromide–NaH solution *via* a cannula and the solution was stirred for 1 h at ambient temperature. At this point, the solution was heated to reflux (65 °C) under partial vacuum overnight. The solution was then cooled to ambient temperature and brine (100 ml) was added slowly. The product was extracted into diethyl ether (3 × 150 ml), dried over sodium sulfate and the solvent was removed under reduced pressure to leave a dark yellow oil (crude yield = 2.89 g), which contained product and (*R*)-2-phenylglycinol in a ratio of 1 : 0.15. This crude product was purified by Kügelrohr distillation at rotary pump vacuum to remove unreacted (*R*)-2-phenylglycinol (125 °C), and the product, a slightly yellow liquid (195 °C). Purified yield = 2.25 g, 9.8 mmol, 71%.

^{1}H NMR (400 MHz, 298 K, $CDCl_3$) δ_H 8.56 (1H, d, $^3J_{HH}$ = 5.0 Hz, Py), 7.69 (1H, td, $^3J_{HH}$ = 8.0 Hz, $^4J_{HH}$ = 2.0 Hz, Py), 7.42–7.18 (7H, m, Ph/Py), 4.70 (2H, s, CH_2Py), 4.31 (1H, dd, $^3J_{HH}$ = 4.5 Hz, 9.0 Hz, CH), 3.71 (1H, dd, $^2J_{HH}$ = 9.0 Hz , $^3J_{HH}$ = 4.5 Hz, CH_2), 3.38 (1H, t, $^2J_{HH}/^3J_{HH}$ = 9.0 Hz, CH_2), 1.83 (2H, s, NH_2).

$^{13}C\{^1H\}$ NMR (100 MHz, 298 K, $CDCl_3$) δ_C 158.4 (Py), 149.2, 142.4, 136.6, 128.5, 127.5, 126.9, 122.4, 121.4 (Ar), 77.3 (CH_2), 74.1 (CH_2Py), 55.6 (CH).

MS (ESI) m/z 212.0 $[M - NH_2]^+$, 229.0 $[M + H]^+$, 251.0 $[M + Na]^+$.

IR ν cm^{-1} 3027 w, 2858 w, 1591 m, 1571 m, 1435 m, 1355 m, 1113 s, 755 s, 700 s.

Elemental Analysis found (Calculated for $C_{14}H_{16}N_2O$) % C 73.76 (73.66), H 7.15 (7.06), N 12.21 (12.27).

Optical rotation −22.11° (6.640 g per 100 ml).

3-(Bromomethyl)pyridine hydrobromide[50]

3-(Hydroxymethyl)pyridine (2.00 g, 18.33 mmol) was dissolved in hydrobromic acid (20 ml, 48%). The mixture was stirred at reflux for 4 h. The solvent was then removed under reduced pressure to leave a light yellow oil which solidified on standing. The solid was washed with ethanol (3 × 50 ml) and the resulting white solid was dried *in vacuo*. Yield = 2.78 g, 10.99 mmol, 60%.

^{1}H NMR (400 MHz, 298 K, D_2O) δ_H 8.92 (1H, s, Py), 8.75 (1H, d, $^3J_{HH}$ = 6.0 Hz, Py), 8.71 (1H, d, $^3J_{HH}$ = 8.0 Hz, Py), 8.08 (1H, dd, $^3J_{HH}$ = 6.0 Hz, $^3J_{HH}$ = 8.0 Hz, Py), 4.77 (2H, s, CH_2).

$^{13}C\{^1H\}$ NMR (100 MHz, 298 K, D_2O) δ_C 147.3, 141.3, 140.6, 138.9, 127.5 (Py), 26.7 (CH_2).

MS (ESI) m/z 172.0/174.0 $[M + H]^+$.

Elemental Analysis found (Calculated for $C_6H_7Br_2N$) % C 28.58 (28.49), H 2.82 (2.79), N 5.40 (5.54).

2-(Pyridin-3-methoxy)-1-phenylethanamine

(*R*)-2-Phenylglycinol (1.00 g, 7.29 mmol) was dissolved in dry THF (10 ml) and was added dropwise to a stirred suspension of sodium hydride (0.61 g, 25.5 mmol, 3.5 eq.) in dry THF (20 ml). This solution was stirred for 1 h at ambient temperature under partial vacuum. 3-(Bromomethyl)-pyridine hydrobromide (1.75 g, 6.93 mmol, 0.95 eq.) was added as a solid. The solution was stirred for 1 h at ambient temperature and then heated to reflux (65 °C) overnight, all under partial vacuum. The solution was then cooled to ambient temperature and brine (60 ml) was added slowly. The product was extracted into diethyl ether (3 × 150 ml), dried over sodium sulfate and the solvent was removed under reduced pressure to leave a yellow oil, which contained product and (*R*)-2-phenylglycinol in a ratio of 1 : 0.19. This crude product was purified by Kügelrohr distillation at rotary pump vacuum to remove unreacted (*R*)-2-phenylglycinol (125 °C), and the product, a slightly yellow liquid (195 °C). Purified yield = 1.16 g, 5.08 mmol, 73%.

^{1}H NMR (300 MHz, 298 K, $CDCl_3$) δ_H 8.49–8.46 (2H, m, Py), 7.57 (1H, dt, $^3J_{HH}$ = 8.0 Hz, $^4J_{HH}$ = 2.0 Hz, Py), 7.32–7.18 (6H, m, Ph/Py), 4.49 (2H, s, CH_2Py), 4.17 (1H, dd, $^3J_{HH}$ = 4.0 Hz, 9.0 Hz, CH), 3.55 (1H, dd, $^2J_{HH}$ = 9.0 Hz, $^3J_{HH}$ = 4.0 Hz, CH_2), 3.41 (1H, t, $^2J_{HH}/^3J_{HH}$ = 9.0 Hz, CH_2), 1.68 (2H, s, NH_2).

$^{13}C\{^1H\}$ NMR (75 MHz, 298 K, $CDCl_3$) δ_C 149.2, 142.3, 135.3, 133.5, 128.4, 127.5, 126.8, 123.5, 123.4 (Ar), 70.7 (CH_2), 70.0 (CH_2Py), 55.5 (CH).

MS (ESI) m/z 212.1 $[M - NH_2]^+$, 229.1 $[M + H]^+$, 251.1 $[M + Na]^+$.

Elemental Analysis found (Calculated for $C_{14}H_{16}N_2O$) % C 73.81 (73.66), H 6.90 (7.06), N 11.95 (12.27).

Optical rotation −19.98° (6.244 g per 100 ml).

2-(Propargyloxy)-1-phenylethanamine

(*R*)-2-Phenylglycinol (0.50 g, 3.6 mmol) was dissolved in dry THF (15 ml) and was added dropwise to a stirred suspension

Open Access Article. Published on 01 August 2013. Downloaded on 10/17/2025 10:08:07 PM. This article is licensed under a Creative Commons Attribution 3.0 Unported Licence.

of sodium hydride (0.17 g, 7.3 mmol, 2.0 eq.) in dry THF (10 ml). The solution was stirred for 1 h at ambient temperature under partial vacuum. Propargyl bromide (80 wt% in toluene, 0.43 ml, 3.8 mmol, 1.05 eq.) was added dropwise and the solution was stirred for 1 h at ambient temperature under argon. At this point, the solution was heated to reflux (65 °C) under partial vacuum overnight before cooling to ambient temperature, followed by the addition of brine (30 ml). The product was extracted into diethyl ether (4 × 50 ml), dried over sodium sulfate and the solvent was removed under reduced pressure to leave a yellow oil (crude yield = 0.52 g). This crude product was purified by Kügelrohr distillation at rotary pump vacuum to give the product as a clear liquid (95 °C). Purified yield = 0.45 g, 2.6 mmol, 71%.

^{1}H NMR (300 MHz, 298 K, $CDCl_3$) δ_H 7.33–7.16 (5H, m, Ph), 4.17–4.10 (3H, m, CH_2–C≡C and CH), 3.60 (1H, dd, $^2J_{HH}$ = 9.0 Hz, $^3J_{HH}$ = 4.0 Hz, C*H*$_2$CHPh), 3.39 (1H, t, $^2J_{HH}/^3J_{HH}$ = 9.0 Hz, C*H*$_2$CHPh), 2.36 (1H, t, $^4J_{HH}$ = 1.5 Hz, C≡CH), 1.70 (2H, s, NH_2).

^{13}C{^{1}H} NMR (100 MHz, 298 K, $CDCl_3$) δ_C 142.3, 128.5, 127.5, 126.9 (Ph), 79.6 (*C*≡CH), 76.3 (*C*H$_2$CHPh), 74.6 (C≡*C*H), 58.5 (*C*H$_2$–C≡C), 55.4 (*C*HPh).

MS (ESI) *m*/*z* 159.0 [M − NH_2]$^+$, 176.0 [M + H]$^+$, 198.0 [M − Na]$^+$, 214.0 [M + K]$^+$.

IR ν cm^{-1} 3289 w, 2857 w, 1604 w, 1493 w, 1453 m, 1356 m, 1088 s, 1020 m, 860 m, 759 s, 699 s.

Elemental Analysis found (Calculated for $C_{11}H_{13}NO$) % C 75.46 (75.40), H 7.56 (7.48), N 7.95 (7.99).

Optical rotation −32.11° (6.082 g per 100 ml).

Benzyl azide[51]

Benzyl bromide (2.0 ml, 16.84 mmol, 1.0 eq.) was dissolved in DMSO (40 ml). Sodium azide (1.64 g, 25.26 mmol, 1.5 eq.) was added as a solid and the reaction was stirred overnight at ambient temperature. Water (75 ml) was added slowly (exothermic) before extracting the product into diethyl ether (3 × 150 ml). The combined diethyl ether layers were washed with brine (2 × 150 ml), dried over sodium sulfate and the solvent removed under reduced pressure to leave a clear colourless oil. Yield = 1.63 g, 12.24 mmol, 73%.

^{1}H NMR (400 MHz, 298 K, $CDCl_3$) δ_H 7.42–7.32 (5H, m, Ph), 4.35 (2H, s, CH_2).

^{13}C{^{1}H} NMR (100 MHz, 298 K, $CDCl_3$) δ_C 135.4, 128.9, 128.3, 128.2 (Ar), 54.8 (CH_2).

MS (EI/CI) *m*/*z* 105.1 [M − 2N]$^+$.

IR ν cm^{-1} 2090 s, 1497 w, 1455 m, 1253 m, 876 w, 735 m, 696 s.

Elemental Analysis found (Calculated for $C_7H_7N_3$) % C 63.53 (63.14), H 5.72 (5.30), N 31.34 (31.56).

3,5-Dimethylbenzyl azide

Using a similar procedure to that for benzyl azide, 3,5-dimethylbenzyl bromide (4.29 g, 21.55 mmol, 1.0 eq.) was dissolved in DMSO (50 ml). Sodium azide (2.13 g, 32.76 mmol, 1.5 eq.) was added as a solid and the reaction was stirred overnight at ambient temperature. Water (80 ml) was added slowly (exothermic) before extracting the product into diethyl ether (3 × 150 ml). The combined diethyl ether layers were washed with brine (2 × 150 ml), dried over sodium sulfate and the solvent removed under reduced pressure to leave a clear colourless oil. Yield = 2.68 g, 16.63 mmol, 77%.

^{1}H NMR (300 MHz, 298 K, $CDCl_3$) δ_H 6.85 (1H, s, Ph), 6.80 (2H, s, Ph), 4.11 (2H, s, CH_2), 2.21 (6H, s, CH_3).

^{13}C{^{1}H} NMR (75 MHz, 298 K, $CDCl_3$) δ_C 138.4, 135.3, 129.9, 126.1 (Ph), 54.8 (CH_2), 21.1 (CH_3).

MS (EI/CI) *m*/*z* 119.1 [M − N_3]$^+$, 133.1 [M − N_2]$^+$, 162.0 [M + H]$^+$.

IR ν cm^{-1} 3018 w, 2920 w, 2873 w, 2092 s, 1608 m, 1463 w, 1378 w, 1343 m, 1243 m, 1164 w, 1039 w, 940 w, 875 w, 840 s, 725 m, 689 m.

Elemental Analysis found (Calculated for $C_9H_{11}N_3$) % C 67.11 (67.04), H 7.14 (6.89), N 26.19 (26.07).

4-Nitrobenzyl azide

Using a similar procedure to that for benzyl azide, 4-nitrobenzyl bromide (2.00 g, 9.26 mmol, 1.0 eq.) was dissolved in DMSO (25 ml). Sodium azide (0.90 g, 13.89 mmol, 1.5 eq.) was added as a solid and the reaction was stirred overnight at ambient temperature. Water (60 ml) was added slowly (exothermic) before extracting the product into diethyl ether (3 × 150 ml). The combined diethyl ether layers were washed with brine (2 × 150 ml), dried over sodium sulfate and the solvent removed under reduced pressure to leave a yellow-orange oil. Yield = 1.54 g, 8.64 mmol, 93%.

^{1}H NMR (400 MHz, 298 K, $CDCl_3$) δ_H 8.24 (2H, d, $^3J_{HH}$ = 8.5 Hz, Ph), 7.50 (2H, d, $^3J_{HH}$ = 8.5 Hz, Ph), 4.50 (2H, s, CH_2).

^{13}C{^{1}H} NMR (100 MHz, 298 K, $CDCl_3$) δ_C 147.9, 142.8, 128.7, 124.2 (Ph), 53.9 (CH_2).

MS (ESI) *m*/*z* 166.1 [M − N + H_2]$^+$.

Elemental Analysis found (Calculated for $C_7H_6N_4O_2$) % C 47.74 (47.19), H 3.35 (3.39), N 30.82 (31.45).

5-(2-Pyridinyloxy)picolinaldehyde

2-(Bromomethyl)pyridine hydrobromide (0.5 g, 1.97 mmol) was dissolved in DMF (10 ml). Potassium carbonate (0.68 g, 4.92 mmol) was added followed by 5-hydroxypicolinaldehyde (0.24 g, 1.97 mmol) and the mixture was stirred at 100 °C for 16 h. The solvent was removed under reduced pressure to give a dark brown solid which was extracted with chloroform (3 × 50 ml), washed with NaOH solution (1 M, 3 × 100 ml) and saturated brine solution (3 × 100 ml) and dried over $MgSO_4$ before evaporation under reduced pressure to give a light brown solid (0.31 g, 1.44 mmol, 73%).

^{1}H-NMR (300 MHz, 298 K, $CDCl_3$): δ 9.99 (s, 1H, CHO), 8.62 (d, 1H, $^3J_{HH}$ = 4.27 Hz, Py), 8.54 (d, 1H, $^3J_{HH}$ = 2.59 Hz, Py), 7.94 (d, 1H, $^3J_{HH}$ = 8.54 Hz, Py), 7.75 (td, 1H, $^3J_{HH}$ = 8.08 Hz, $^4J_{HH}$ = 1.52 Hz, Py), 7.51 (d, 1H, $^3J_{HH}$ = 8.08 Hz, Py), 7.39 (dd, 1H, $^3J_{HH}$ = 8.54 Hz, $^4J_{HH}$ = 2.74 Hz, Py), 7.29 (dd, 1H, $^3J_{HH}$ = 7.47 Hz, $^4J_{HH}$ = 4.73 Hz, Py), 5.33 (s, 2H, CH_2).

^{13}C-NMR (101 MHz, 298 K, $CDCl_3$); δ 192.1 (CHO), 158.0, 155.5, 149.7, 146.8, 139.3, 137.2, 123.5, 123.4, 121.7, 121.2 (Py), 71.43 (CH_2).

 This journal is © The Royal Society of Chemistry 2013

Open Access Article. Published on 01 August 2013. Downloaded on 10/17/2025 10:08:07 PM. This article is licensed under a Creative Commons Attribution 3.0 Unported Licence.

ESI-MS – 215 $[M + H]^+$, 237 $[M + Na]^+$.

Elemental Analysis found (Calculated for $C_{12}H_{10}N_2O_2$) C 66.16% (67.28%), H 4.48% (4.70%), N 12.86% (13.07%).

5-(3-Pyridinyloxy)picolinaldehyde

Using a similar procedure as for 5-(2-pyridinyloxy)picolinaldehyde, 3-(bromomethyl)pyridine hydrobromide (0.5 g, 1.97 mmol) gave a light brown solid (0.382 g, 1.78 mmol, 44%).

^{1}H NMR (400 MHz, 298 K, $CDCl_3$): δ_H 10.00 (s, 1H, CHO), 8.72 (s, 1H, Py), 8.65 (1H, d, $^3J_{HH}$ = 5.0 Hz), 8.51 (1H, d, $^3J_{HH}$ = 2.5 Hz, Py), 7.97 (1H, d, $^3J_{HH}$ = 8.5 Hz, Py), 7.78 (1H, d, $^3J_{HH}$ = 8.0 Hz, Py), 7.37 (2H, m Py), 5.22 (2H, s, CH_2).

^{13}C NMR (101 MHz, 298 K, $CDCl_3$): δ_C 196.0 (CHO), 192.0, 187.3, 162.6, 150.2, 149.1, 138.9, 135.4, 123.7, 123.3, 121.1 (Py), 68.24 (CH_2).

ESI-MS: 215 $[M + H]^+$, 237 $[M + Na]^+$.

Elemental Analysis found (Calculated for $C_{12}H_{10}N_2O_2$) C 67.28% (67.28%), H 4.62% (4.70%), N 12.55% (13.07%).

5-(Propargyloxy)picolinaldehyde

Potassium carbonate (0.59 g, 4.26 mmol) was added to a solution of 5-(hydroxy)picolinaldehyde (0.50 g, 4.06 mmol) in acetonitrile (40 ml). Propargyl bromide (80 wt% in toluene, 0.475 ml) was added. The solution was stirred at reflux temperature (*ca.* 85 °C) overnight before allowing to cool to ambient temperature and passing a short column of silica, eluting with acetonitrile until the product was fully removed (TLC). This left a brown band at the top of the column. The solvent was evaporated and the crude product was dissolved in dichloromethane, filtered and evaporated under reduced pressure to leave a dark orange oil which was dried overnight *in vacuo*. Yield = 0.45 g, 2.79 mmol, 69%.

^{1}H NMR (400 MHz, 298 K, DMSO) δ_H 9.90 (1H, s, HC═O), 8.53 (1H, d, $^4J_{HH}$ = 3.0 Hz, Py), 7.97 (1H, d, $^3J_{HH}$ = 8.5 Hz, Py), 7.64 (1H, dd, $^3J_{HH}$ = 8.5 Hz, $^4J_{HH}$ = 3.0 Hz, Py), 5.05 (2H, d, $^4J_{HH}$ = 2.5 Hz, CH_2–C≡C), 3.71 (1H, t, $^4J_{HH}$ = 2.5 Hz, C≡CH).

^{13}C{^{1}H} NMR (100 MHz, 298 K, DMSO) δ_C 191.9 (CO), 156.7, 146.1, 138.8, 123.3, 121.7 (Py), 79.4 (*C*≡CH), 78.9 (C≡*C*H), 56.3 (CH_2).

MS (ESI) *m*/*z* 162.2 $[M + H]^+$, 184.1 $[M + Na]^+$.

IR ν cm^{-1} 3213 w, 2127 w, 1692 s, 1569 s, 1490 w, 1474 w, 1379 w, 1308 m, 1282 w, 1259 s, 1203 s, 1132 m, 1006 s, 975 m, 916 w, 835 s, 800 s, 762 m, 732 m, 694 s, 659 s.

Elemental Analysis found (Calculated for $C_9H_7NO_2$) % C 66.85 (67.07), H 4.02 (4.38), N 8.52 (8.69).

fac,Δ_{Fe},R_C-[Fe**L**$^1{}_3$](ClO$_4$)$_2$

2-Pyridinecarboxaldehyde (0.32 g, 3.0 mmol, 3.0 eq.) and (*R*)-2-(pyridin-2-methoxy)-1-phenylethanamine (0.68 g, 3.0 mmol, 3.0 eq.) were dissolved in acetonitrile (15 ml) to form a yellow solution. Iron(II) perchlorate hexahydrate (0.36 g, 1.0 mmol, 1.0 eq.) in acetonitrile (5 ml) was added to give a purple solution. This was stirred overnight at ambient temperature before the solvent was removed under reduced pressure. The product, [Fe**L**$^1{}_3$](ClO$_4$)$_2$, was recrystallised from acetonitrile and ethyl acetate and the resulting purple crystals were filtered and dried *in vacuo*. Yield = 0.59 g, 0.49 mmol, 49%. Single crystals were grown from acetonitrile–methanol.

^{1}H NMR (400 MHz, 298 K, CD_3CN) δ_H 9.03 (3H, s, HC═N), 8.60 (3H, d, $^3J_{HH}$ = 5.5 Hz, Py), 7.77 (3H, td, $^3J_{HH}$ = 8.0 Hz, $^4J_{HH}$ = 2.0 Hz, Py), 7.68 (3H, td, $^3J_{HH}$ = 8.0 Hz, $^4J_{HH}$ = 1.5 Hz, Py), 7.61 (3H, d, $^3J_{HH}$ = 8.0 Hz, Py), 7.40 (3H, d, $^3J_{HH}$ = 8.0 Hz, Py), 7.28 (3H, t, $^3J_{HH}$ = 6.0 Hz, Py), 7.16 (3H, td, $^3J_{HH}$ = 6.0 Hz, $^4J_{HH}$ = 1.5 Hz, Py), 7.03 (3H, t, $^3J_{HH}$ = 7.0 Hz, Ph), 6.86 (6H, t, $^3J_{HH}$ = 7.0 Hz, Ph), 6.75 (3H, d, $^3J_{HH}$ = 6.0 Hz, Py), 6.65 (6H, d, $^3J_{HH}$ = 7.0 Hz, Ph), 5.85 (3H, dd, $^3J_{HH}$ = 10.5 Hz, $^3J_{HH}$ = 3.5 Hz, CH), 4.95 (3H, d, $^2J_{HH}$ = 13.0 Hz, CH_2Py), 4.89 (3H, d, $^2J_{HH}$ = 13.0 Hz, CH_2Py), 4.35 (3H, t, $^2J_{HH}$/$^3J_{HH}$ = 10.5 Hz, CH_2), 3.50 (3H, dd, $^2J_{HH}$ = 10.5 Hz, $^3J_{HH}$ = 3.5 Hz, CH_2).

^{13}C{^{1}H} NMR (100 MHz, 298 K, CD_3CN) δ_C 171.6 (C═N), 158.5, 157.2, 153.4, 149.4, 138.3, 136.9, 134.6, 129.0, 128.8, 127.8, 127.5, 125.8, 123.0, 122.4 (Ar), 74.2 (*C*H$_2$Py), 72.5 (CH*C*H$_2$), 71.1 (CH).

MS (ESI) *m*/*z* 503.70 [Fe**L**$^1{}_3$]$^{2+}$.

IR ν cm^{-1} 1733 m, 1590 m, 1473 m, 1353 w, 1245 m, 1077 s, 760 s, 700 s.

Elemental Analysis found (Calculated for $C_{60}H_{57}Cl_2FeN_9O_{11}$) % C 59.17 (59.71), H 4.88 (4.76), N 9.92 (10.44).

Crystallography. *fac*,Δ_{Fe},R_C-[Fe**L**$^1{}_3$](ClO$_4$)$_2$·1.5MeOH $C_{61.5}H_{63}Cl_2FeN_9O_{12.5}$, *M* = 1254.96, cubic, $P2_13$, red block 0.34 × 0.24 × 0.15 mm, *a* = 18.4606(2), *b* = 18.4606(2), *c* = 18.4606(2) Å, α = 90°, β = 90°, γ = 90°, *U* = 6291.26(12) Å^3, *Z* = 4, *T* = 273(2) K, radiation Mo-Kα (λ = 0.71073 Å), 18 110 total reflections, 4777 unique (R_{int} = 0.0790), R_1 = 0.0798 (obs. data), wR_2 = 0.2101 (all data), GooF 1.027, Flack 0.07(4).

Δ_{Fe},Δ_{Cu},R_C-[Fe**L**$^1{}_3$Cu](ClO$_4$)$_2$I

fac,Δ_{Fe},R_C-[Fe**L**$^1{}_3$](ClO$_4$)$_2$ (0.20 g, 0.17 mmol) was dissolved in acetonitrile (15 ml). Copper(I) iodide (32 mg, 0.17 mmol) was dissolved in acetonitrile (10 ml) and was added. The solution was stirred overnight at ambient temperature. The solvent was then removed under reduced pressure and the crude purple solid was recrystallised from acetonitrile–ethyl acetate. Yield = 0.13 g, 0.093 mmol, 55%.

^{1}H NMR (400 MHz, 298 K, CD_3CN) δ_H 9.05 (3H, s, HC═N), 8.68 (3H, d, $^3J_{HH}$ = 5 Hz, Py), 7.81 (3H, t, $^3J_{HH}$ = 8 Hz, Py), 7.68 (3H, t, $^3J_{HH}$ = 8 Hz, Py), 7.62 (3H, d, $^3J_{HH}$ = 8 Hz, Py), 7.40 (3H, d, $^3J_{HH}$ = 8 Hz, Py), 7.33 (3H, t, $^3J_{HH}$ = 6 Hz, Py), 7.15 (3H, t, $^3J_{HH}$ = 6 Hz, Py), 7.04 (3H, t, $^3J_{HH}$ = 7 Hz, Ph), 6.88 (6H, t, $^3J_{HH}$ = 8 Hz, Ph), 6.73 (3H, d, $^3J_{HH}$ = 5 Hz, Py), 6.64 (6H, d, $^3J_{HH}$ = 7 Hz, Ph), 5.79 (3H, dd, $^3J_{HH}$ = 10 Hz, $^3J_{HH}$ = 2 Hz, CH), 5.02 (3H, d, $^2J_{HH}$ = 13 Hz, CH_2Py), 4.82 (3H, d, $^2J_{HH}$ = 13 Hz, CH_2Py), 4.34 (3H, t, $^2J_{HH}$/$^3J_{HH}$ = 11 Hz, CH_2), 3.46 (3H, dd, $^2J_{HH}$ = 11 Hz, $^3J_{HH}$ = 2 Hz, CH_2).

^{13}C{^{1}H} NMR (100 MHz, 298 K, CD_3CN) δ_C 172.5 (C═N), 159.5, 158.1, 154.4, 150.5, 139.3, 138.0, 135.5, 130.0, 129.9, 128.9, 128.5, 126.8, 124.1, 123.6 (Py/Ph), 75.1 (*C*H$_2$Py), 73.5 (CH*C*H$_2$), 72.1 (CH).

MS (ESI) *m*/*z* 503.7 [Fe**L**$^1{}_3$]$^{2+}$, 318.2 [**L**^{1} + H]$^+$.

IR ν cm^{-1} 3055 w, 2868 w, 1641 w, 1592 m, 1571 w, 1495 w, 1475 m, 1437 m, 1388 w, 1358 w, 1302 w, 1239 w, 1048 s, 835 m, 759 s, 700 s.

Open Access Article. Published on 01 August 2013. Downloaded on 10/17/2025 10:08:07 PM. This article is licensed under a Creative Commons Attribution 3.0 Unported Licence.

Elemental Analysis found (Calculated for $C_{60}H_{57}Cl_2CuFeIN_9O_{11}$) % C 51.79 (51.57), H 4.02 (4.11), N 9.31 (9.02).

Δ_{Fe},R_C-[Fe$\mathbf{L^1}_3$Ag(CH$_3$CN)](ClO$_4$)$_3$

fac,Δ_{Fe},R_C-[Fe$\mathbf{L^1}_3$](ClO$_4$)$_2$ (0.05 g, 0.04 mmol) was dissolved in acetonitrile (15 ml). Silver(I) perchlorate (8.6 mg, 0.04 mmol) was added as a solid. The solution was stirred overnight at ambient temperature. The solvent was then removed under reduced pressure and the crude purple solid was recrystallised from acetonitrile–ethyl acetate. Yield = 0.04 g, 0.028 mmol, 71%.

^{1}H NMR (400 MHz, 298 K, CD$_3$CN) δ_H 9.06 (3H, s, HC═N), 8.75 (3H, dd, $^3J_{HH}$ = 5.0 Hz, $^4J_{HH}$ = 1.0 Hz, Py), 7.98 (3H, td, $^3J_{HH}$ = 7.5 Hz, $^4J_{HH}$ = 1.5 Hz, Py), 7.83 (3H, d, $^3J_{HH}$ = 7.5 Hz, Py), 7.64 (3H, td, $^3J_{HH}$ = 7.5 Hz, $^4J_{HH}$ = 1.5 Hz, Py), 7.50 (3H, m, Py), 7.42 (3H, d, $^3J_{HH}$ = 7.5 Hz, Py), 7.11 (3H, m, Py), 7.05 (3H, t, $^3J_{HH}$ = 7.5 Hz, Ph), 6.94 (6H, t, $^3J_{HH}$ = 7.5 Hz, Ph), 6.72 (3H, d, $^3J_{HH}$ = 5.5 Hz, Py), 6.49 (6H, d, $^3J_{HH}$ = 7.5 Hz, Ph), 5.84 (3H, dd, $^3J_{HH}$ = 11.5 Hz, $^3J_{HH}$ = 3.0 Hz, CH), 4.97 (3H, d, $^2J_{HH}$ = 11.5 Hz, CH$_2$Py), 4.76 (3H, d, $^2J_{HH}$ = 11.5 Hz, CH$_2$Py), 4.35 (3H, t, $^2J_{HH}$/$^3J_{HH}$ = 11.5 Hz, CH$_2$), 3.46 (3H, dd, $^2J_{HH}$ = 11.5 Hz, $^3J_{HH}$ = 3.0 Hz, CH$_2$).

^{13}C{^{1}H} NMR (100 MHz, 298 K, CD$_3$CN) δ_C 172.0 (C═N), 159.4, 156.9, 154.4, 153.1, 140.5, 139.4, 134.9, 130.3, 130.2, 129.2, 128.6, 126.6, 126.5, 125.9 (Ar), 74.7 (*C*H$_2$Py), 73.7 (CH*C*H$_2$), 71.4 (CH).

MS (ESI) *m*/*z* 503.7 [Fe$\mathbf{L^1}_3$]$^{2+}$, 345.1 [Fe$\mathbf{L^1}_2$]$^{2+}$.

Elemental Analysis found (Calculated for $C_{62}H_{60}AgCl_3FeN_{10}O_{15}$) % C 51.43 (51.17), H 4.01 (4.16), N 9.27 (9.62).

fac,Δ_{Fe},R_C-[Fe$\mathbf{L^2}_3$](ClO$_4$)$_2$

2-Pyridinecarboxaldehyde (0.33 g, 3.0 mmol) and (*R*)-2-(pyridin-3-methoxy)-1-phenylethanamine (0.70 g, 3.0 mmol) were dissolved in acetonitrile (15 ml) to form a yellow solution. Iron(II) perchlorate hexahydrate (0.37 g, 1.0 mmol) in acetonitrile (5 ml) was added and immediately the solution turned purple. This was stirred overnight at ambient temperature before the solvent was removed under reduced pressure. The product, [Fe$\mathbf{L^2}_3$](ClO$_4$)$_2$, was recrystallised from acetonitrile and ethyl acetate and the resulting purple crystals were filtered and dried *in vacuo*. Yield = 0.86 g, 0.71 mmol, 71%.

^{1}H NMR (400 MHz, 298 K, CD$_3$CN) δ_H 8.97 (3H, br s, Py), 8.94 (3H, s, HC═N), 8.53 (3H, br s, Py), 7.96 (3H, d, $^3J_{HH}$ = 7.5 Hz, Py), 7.65 (3H, t, $^3J_{HH}$ = 7.5 Hz, Py), 7.39–7.35 (6H, m, Py), 7.11 (3H, t, $^3J_{HH}$ = 6.5 Hz, Py), 7.04 (3H, t, $^3J_{HH}$ = 7.5 Hz, Ph), 6.89 (6H, t, $^3J_{HH}$ = 7.5 Hz, Ph), 6.66 (3H, d, $^3J_{HH}$ = 5.5 Hz, Py), 6.53 (6H, d, $^3J_{HH}$ = 7.5 Hz, Ph), 5.72 (3H, dd, $^3J_{HH}$ = 11.0 Hz, $^3J_{HH}$ = 3.0 Hz, CH), 4.86 (3H, d, $^2J_{HH}$ = 11.5 Hz, CH$_2$Py), 4.82 (3H, d, $^2J_{HH}$ = 11.5 Hz, CH$_2$Py), 4.22 (3H, t, $^2J_{HH}$/$^3J_{HH}$ = 11.0 Hz, CH$_2$), 3.18 (3H, dd, $^2J_{HH}$ = 11.0 Hz, $^3J_{HH}$ = 3.0 Hz, CH$_2$).

^{13}C{^{1}H} NMR (100 MHz, 298 K, CD$_3$CN) δ_C 172.1 (C═N), 159.5, 154.5, 147.0, 139.4, 137.4, 135.6, 130.1, 130.0, 129.1, 128.5, 127.8, 126.8, 126.7, 124.8 (Ar), 73.3 (CH$_2$), 72.3 (CH), 72.1 (*C*H$_2$Py).

MS (ESI) *m*/*z* 503.70 [Fe$\mathbf{L^n}_3$]$^{2+}$, 318.1 [L + H]$^+$.

Elemental Analysis found (Calculated for $C_{60}H_{57}Cl_2FeN_9O_{11}$) % C 59.24 (59.71), H 4.85 (4.76), N 10.01 (10.44).

Δ_{Fe},Δ_{Cu},R_C-[Fe$\mathbf{L^2}_3$CuI](ClO$_4$)$_2$

fac,Δ_{Fe},R_C-[Fe$\mathbf{L^2}_3$](ClO$_4$)$_2$ (50.0 mg, 0.0414 mmol) was dissolved in acetonitrile (10 ml). Copper(I) iodide (7.9 mg, 0.0414 mmol) was added as a solid to the reaction. The solution was stirred overnight at ambient temperature. The solvent was then removed under reduced pressure and the crude purple solid was recrystallised from acetonitrile–ethyl acetate. Yield = 48 mg, 0.0344 mmol, 83%.

^{1}H NMR (400 MHz, 298 K, CD$_3$CN) δ_H 8.94 (3H, s, HC═N), 8.66 (3H, br s, Py), 8.00 (3H, br s, Py), 7.79 (3H, br s, Py), 7.68 (3H, td, $^3J_{HH}$ = 7.5 Hz, $^4J_{HH}$ = 1.0 Hz, Py), 7.41 (3H, d, $^3J_{HH}$ = 7.5 Hz, Py), 7.26 (3H, br s, Py), 7.16–7.13 (3H, m, Py), 7.06 (3H, t, $^3J_{HH}$ = 7.5 Hz, Ph), 6.92 (6H, t, $^3J_{HH}$ = 7.5 Hz, Ph), 6.69 (3H, d, $^3J_{HH}$ = 5.5 Hz, Py), 6.59 (6H, d, $^3J_{HH}$ = 7.5 Hz, Ph), 5.67 (3H, d, $^3J_{HH}$ = 9.5 Hz, CH), 5.02 (3H, br s, CH$_2$Py), 4.78 (3H, br s, CH$_2$Py), 4.14 (3H, t, $^2J_{HH}$/$^3J_{HH}$ = 10.0 Hz, CH$_2$), 3.36 (3H, d, $^2J_{HH}$ = 10.0 Hz, CH$_2$).

^{13}C{^{1}H} NMR (100 MHz, 298 K, CD$_3$CN) δ_C 172.9 (C═N), 160.2, 155.1, 140.1, 136.1, 130.8, 130.7, 129.7, 129.2, 127.5 (Ar), 73.5 (CH$_2$), 72.9 (CH), 72.3 (*C*H$_2$Py). Note that the Cu-coordinated pyridine C atoms were not detected; the H signals are broad in ^{1}H NMR spectrum.

MS (ESI) *m*/*z* 503.7 [Fe$\mathbf{L^2}_3$]$^{2+}$, 345.1 [Fe$\mathbf{L^2}_2$]$^{2+}$, 318.1 [$\mathbf{L^2}$+H]$^+$.

Elemental Analysis found (Calculated for $C_{60}H_{57}Cl_2CuFeIN_9O_{11}$) % C 51.41 (51.57), H 4.04 (4.11), N 9.19 (9.02).

Δ_{Fe},R_C-[Fe$\mathbf{L^2}_3$Ag(CH$_3$CN)](ClO$_4$)$_3$

fac,Δ_{Fe},R_C-[Fe$\mathbf{L^2}_3$](ClO$_4$)$_2$ (50.0 mg, 0.0414 mmol) was dissolved in acetonitrile (10 ml). Silver(I) perchlorate (8.6 mg, 0.0414 mmol) was added as a solid to the reaction. The solution was stirred overnight at ambient temperature. The solvent was then removed under reduced pressure and the crude purple solid was recrystallised from acetonitrile–ethyl acetate. Yield = 52 mg, 0.0368 mmol, 89%.

^{1}H NMR (400 MHz, 298 K, CD$_3$CN) δ_H 8.93 (3H, s, HC═N), 8.82 (3H, s, Py), 8.53 (3H, d, $^3J_{HH}$ = 3.5 Hz, Py), 7.94 (3H, d, $^3J_{HH}$ = 7.5 Hz, Py), 7.67 (3H, td, $^3J_{HH}$ = 7.5 Hz, $^4J_{HH}$ = 1.5 Hz, Py), 7.41–7.39 (6H, m, Py), 7.13 (3H, m, Py), 7.05 (3H, t, $^3J_{HH}$ = 7.5 Hz, Ph), 6.91 (6H, t, $^3J_{HH}$ = 7.5 Hz, Ph), 6.67 (3H, d, $^3J_{HH}$ = 5.5 Hz, Py), 6.57 (6H, d, $^3J_{HH}$ = 7.5 Hz, Ph), 5.68 (3H, dd, $^3J_{HH}$ = 10.5 Hz, $^3J_{HH}$ = 3.0 Hz, CH), 4.90 (3H, d, $^2J_{HH}$ = 11.5 Hz, CH$_2$Py), 4.75 (3H, d, $^2J_{HH}$ = 11.5 Hz, CH$_2$Py), 4.19 (3H, t, $^2J_{HH}$/$^3J_{HH}$ = 10.5 Hz, CH$_2$), 3.28 (3H, dd, $^2J_{HH}$ = 10.5 Hz, $^3J_{HH}$ = 3.0 Hz, CH$_2$).

^{13}C{^{1}H} NMR (100 MHz, 298 K, CD$_3$CN) δ_C 172.9 (C═N), 160.2, 155.1, 153.4, 140.1, 138.8, 136.2, 130.8, 130.7, 130.6, 129.7, 129.2, 127.8, 127.4, 125.7 (Ar), 73.7 (CH$_2$), 72.9 (CH), 72.4 (*C*H$_2$Py).

MS (ESI) *m*/*z* 503.7 [Fe$\mathbf{L^2}_3$]$^{2+}$, 345.1 [Fe$\mathbf{L^2}_2$]$^{2+}$, 318.1 [$\mathbf{L^2}$ + H]$^+$.

Elemental Analysis found (Calculated for $C_{62}H_{60}AgCl_3FeN_{10}O_{15}$) % C 51.24 (51.17), H 4.11 (4.16), N 9.41 (9.62).

 This journal is © The Royal Society of Chemistry 2013

Open Access Article. Published on 01 August 2013. Downloaded on 10/17/2025 10:08:07 PM. This article is licensed under a Creative Commons Attribution 3.0 Unported Licence.

fac,Δ_{Fe},R_C-[Fe$\mathbf{L}^3{}_3$](ClO$_4$)$_2$

2-Pyridinecarboxaldehyde (0.33 g, 3.0 mmol) and (*R*)-2-(propargyloxy)-1-phenylethanamine (0.52 g, 3.0 mmol) were dissolved in acetonitrile (15 ml) to form a yellow solution. Iron(II) perchlorate hexahydrate (0.37 g, 1.0 mmol) in acetonitrile (5 ml) was added and immediately the solution turned purple. This was stirred overnight at ambient temperature before the solvent was removed under reduced pressure. The product, [Fe$\mathbf{L}^3{}_3$](ClO$_4$)$_2$, was recrystallised from acetonitrile and ethyl acetate and the resulting purple crystals were filtered and dried *in vacuo*. Yield = 0.81 g, 0.77 mmol, 77%.

^{1}H NMR (400 MHz, 298 K, CD$_3$CN) δ_H 8.93 (3H, s, HC=N), 7.70 (3H, td, $^3J_{HH}$ = 8.0 Hz, $^4J_{HH}$ = 1.5 Hz, Py), 7.40 (3H, d, $^3J_{HH}$ = 7.5 Hz, Py), 7.18 (3H, td, $^3J_{HH}$ = 7.5 Hz, $^4J_{HH}$ = 1.5 Hz, Py), 7.10 (3H, t, $^3J_{HH}$ = 7.0 Hz, Ph), 6.99 (6H, t, $^3J_{HH}$ = 7.0 Hz, Ph), 6.78 (9H, m, Py/Ph), 5.81 (3H, dd, $^3J_{HH}$ = 11.0 Hz, $^3J_{HH}$ = 3.5 Hz, CH), 4.60 (3H, dd, $^2J_{HH}$ = 16.0 Hz, $^4J_{HH}$ = 2.0 Hz, CH$_2$–C≡C), 4.51 (3H, dd, $^2J_{HH}$ = 16.0 Hz, $^4J_{HH}$ = 2.0 Hz, CH$_2$–C≡C), 4.38 (3H, t, $^2J_{HH}$/$^3J_{HH}$ = 11.0 Hz, C*H*$_2$CHPh), 3.70 (3H, dd, $^2J_{HH}$ = 11.0 Hz, $^3J_{HH}$ = 3.5 Hz, C*H*$_2$CHPh), 2.95 (3H, t, $^4J_{HH}$ = 2.0 Hz, C≡CH).

^{13}C{^{1}H} NMR (100 MHz, 298 K, CD$_3$CN) δ_C 170.9 (C=N), 158.1, 153.3, 138.2, 134.1, 128.8, 128.8, 127.8, 127.4, 125.6 (Ph), 78.7 (*C*≡CH), 76.0 (C≡*C*H), 70.9 (*C*H$_2$CHPh), 70.4 (*C*HPh), 58.0 (*C*H$_2$–C≡C).

MS (ESI) *m*/*z* 424.16 [Fe$\mathbf{L}^3{}_3$]$^{2+}$.

IR ν cm^{-1} 3259 w, 1732 w, 1613 w, 1474 m, 1452 m, 1356 w, 1240 m, 1076 s, 758 s, 699 s.

Elemental Analysis found (Calculated for C$_{51}$H$_{48}$Cl$_2$FeN$_6$O$_{11}$) % C 57.36 (58.47), H 4.65 (4.62), N 7.69 (8.02).

Δ_{Fe},Λ_{Cu},R_C-[Fe$\mathbf{L}^4{}_3$Cu](ClO$_4$)$_2$I

fac,Δ_{Fe},R_C-[Fe$\mathbf{L}^3{}_3$](ClO$_4$)$_2$·H$_2$O (0.25 g, 0.24 mmol) was dissolved in dry acetonitrile (30 ml) in a Schlenk vessel. Dry triethylamine (0.10 ml, 0.72 mmol) was added, followed by benzyl azide (95 mg, 0.72 mmol) in dry acetonitrile (10 ml). Finally, copper(I) iodide (45 mg, 0.24 mmol) was added as a solid. The solution remained purple in colour and was stirred for 24 h under argon at ambient temperature. The solvent was removed under reduced pressure and the resultant solid was recrystallised from acetonitrile and ethyl acetate. Yield = 0.21 g, 0.13 mmol, 53%.

^{1}H NMR (400 MHz, 298 K, CD$_3$CN) δ_H 8.85 (3H, s, HC=N), 8.27 (3H, s, triazole CH), 7.58 (3H, t, $^3J_{HH}$ = 7.5 Hz, Py), 7.34 (3H, d, $^3J_{HH}$ = 7.5 Hz, Py), 7.15–6.91 (27H, m, Py/Ph), 6.64 (3H, d, $^3J_{HH}$ = 5.5 Hz, Py), 6.39 (6H, br m, Py/Ph), 5.53 (3H, d, $^2J_{HH}$ = 14.5 Hz, NC*H*$_2$Ph), 5.48 (3H, d, $^2J_{HH}$ = 14.5 Hz, NC*H*$_2$Ph), 5.39 (3H, dd, $^3J_{HH}$ = 11.0 Hz, 2.5 Hz, CH), 4.62 (3H, d, $^2J_{HH}$ = 11.0 Hz, OC*H*$_2$–triazole), 4.36 (3H, d, $^2J_{HH}$ = 11.0 Hz, OC*H*$_2$–triazole), 3.64 (3H, t, $^2J_{HH}$/$^3J_{HH}$ = 11.0 Hz, C*H*$_2$CHPh), 1.39 (3H, br d, $^2J_{HH}$ = 10.0 Hz, C*H*$_2$CHPh).

^{13}C{^{1}H} NMR (100 MHz, 298 K, CD$_3$CN) δ_C 171.5 (C=N), 159.5, 154.2, 145.6, 139.1, 135.5, 135.1, 130.0, 129.8, 129.6, 129.4, 128.9, 128.2, 126.7, 126.6, 126.0 (Ar, triazole *C*H), 72.4 (CH*C*H$_2$), 71.3 (CH), 63.2 (O*C*H$_2$–triazole), 55.5 (N*C*H$_2$Ph).

MS (ESI) *m*/*z* 623.75 [Fe$\mathbf{L}^4{}_3$]$^{2+}$.

IR ν cm^{-1} 3036 w, 1612 w, 1496 w, 1474 w, 1454 m, 1334 w, 1224 w, 1075 s, 821 w, 756 s, 720 s, 700 s.

Elemental Analysis found (Calculated for C$_{72}$H$_{69}$Cl$_2$CuFeIN$_{15}$O$_{11}$) % C 52.75 (52.81), H 4.26 (4.25), N 12.55 (12.83).

Crystallography. *fac*,Δ_{Fe},Λ_{Cu},R_C-[FeCu$\mathbf{L}^4{}_3$](ClO$_4$)$_{2.66}$(I$_3$)$_{0.33}$ C$_{72}$H$_{69}$Cl$_{2.66}$CuFeIN$_{15}$O$_{13.66}$, M = 1703.83, cubic, $P2_13$, purple block 0.35 × 0.28 × 0.25 mm, a = 20.5043(4), b = 20.5043(4), c = 20.5043(4) Å, α = 90°, β = 90°, γ = 90°, U = 8620.6(3) Å^3, Z = 4, T = 100(2) K, radiation Cu-Kα (λ = 1.54184 Å), 18 683 total reflections, 5470 unique (R_{int} = 0.0552), R_1 = 0.0876 (obs. data), wR_2 = 0.2242 (all data), GooF 1.369, Flack 0.012(11).

Δ_{Fe},Λ_{Cu},R_C-[Fe$\mathbf{L}^5{}_3$Cu](ClO$_4$)$_2$I

fac,Δ_{Fe},R_C-[Fe$\mathbf{L}^3{}_3$](ClO$_4$)$_2$·H$_2$O (0.25 g, 0.24 mmol) was dissolved in dry acetonitrile (25 ml) in a Schlenk vessel. Dry triethylamine (0.10 ml, 0.72 mmol) was added, followed by 3,5-dimethylbenzyl azide (0.12 g, 0.72 mmol) in dry acetonitrile (10 ml). Finally, copper(I) iodide (45 mg, 0.24 mmol) was added. The solution remained purple in colour and was stirred for 24 h under argon at ambient temperature. The solvent was removed under reduced pressure and the resultant solid recrystallised from acetonitrile and ethyl acetate. Yield = 0.23 g, 0.13 mmol, 56%.

^{1}H NMR (300 MHz, 298 K, CD$_3$CN) δ_H 8.86 (3H, s, HC=N), 8.27 (3H, s, triazole), 7.59 (3H, t, $^3J_{HH}$ = 7.5 Hz, Py), 7.33 (3H, d, $^3J_{HH}$ = 7.5 Hz, Py), 7.09–7.02 (6H, m, Py/Ph), 6.93–6.89 (6H, m, Py/Ph), 6.80–6.79 (9H, m, Py/Ph), 6.67 (3H, d, $^3J_{HH}$ = 7.5 Hz, Py), 6.31 (6H, br m, Py/Ph), 5.49–5.36 (9H, m, CH and NC*H*$_2$-aryl), 4.63 (3H, d, $^2J_{HH}$ = 11.0 Hz, OC*H*$_2$–triazole), 4.30 (3H, d, $^2J_{HH}$ = 11.0 Hz, OC*H*$_2$–triazole), 3.80 (3H, t, $^2J_{HH}$/$^3J_{HH}$ = 11.0 Hz, C*H*$_2$CHPh), 1.98 (18H, s, CH$_3$), 1.73 (3H, br d, $^2J_{HH}$ = 11.0 Hz, C*H*$_2$CHPh).

^{13}C {^{1}H} NMR (400 MHz, 298 K, CD$_3$CN) δ_C 171.6 (C=N), 159.4, 154.3, 145.5, 139.6, 139.2, 135.4, 134.9, 131.3, 130.1 130.0, 129.9, 128.9, 128.3, 127.2, 126.0 (Ar/triazole *C*H), 72.6 (CH*C*H$_2$), 71.4 (CH$_2$*C*HPh), 63.1 (O*C*H$_2$–triazole), 55.7 (N*C*H$_2$Ph), 21.2 (CH$_3$).

MS (ESI) *m*/*z* 453.2 [Fe$\mathbf{L}^5{}_2$]$^{2+}$, 665.8 [Fe$\mathbf{L}^5{}_3$]$^{2+}$.

IR ν cm^{-1} 3016 w, 2864 w, 1728 m, 1610 m, 1473 m, 1452 m, 1390 m, 1334 m, 1239 m, 1160 w, 1071 s, 1007 m, 835 m, 796 m, 746 s, 701 s.

Elemental Analysis found (calculated for C$_{78}$H$_{81}$Cl$_2$CuFeIN$_{15}$O$_{11}$) % C 54.72 (54.40), H 4.34 (4.74), N 11.86 (12.20).

Δ_{Fe},Λ_{Cu},R_C-[Fe$\mathbf{L}^6{}_3$Cu](ClO$_4$)$_2$I

fac,Δ_{Fe},R_C-[Fe$\mathbf{L}^3{}_3$](ClO$_4$)$_2$·H$_2$O (0.10 g, 0.095 mmol) was dissolved in dry acetonitrile (15 ml) in a Schlenk. Dry triethylamine (0.40 μl, 0.285 mmol) was added to the reaction, followed by 4-nitrobenzyl azide (0.051 g, 0.285 mmol) in dry acetonitrile (10 ml). Finally, copper(I) iodide (18 mg, 0.095 mmol) was added as a solid. The solution remained purple in colour and was stirred for 24 h under argon at ambient temperature. The solvent was removed under reduced pressure and the resultant solid was recrystallised from acetonitrile and ethyl acetate. Yield = 0.23 g, 0.13 mmol, 71%.

Open Access Article. Published on 01 August 2013. Downloaded on 10/17/2025 10:08:07 PM. This article is licensed under a Creative Commons Attribution 3.0 Unported Licence.

^{1}H NMR (400 MHz, 298 K, CD_3CN) δ_H 8.78 (3H, s, HC═N), 8.38 (3H, s, triazole CH), 7.72 (6H, d, $^3J_{HH}$ = 8.5 Hz, Ph–NO_2), 7.55 (3H, td, $^3J_{HH}$ = 7.5 Hz, $^4J_{HH}$ = 1.5 Hz, Py), 7.40 (6H, d, $^3J_{HH}$ = 8.5 Hz, Ph–NO_2), 7.29 (3H, d, $^3J_{HH}$ = 7.5 Hz, Py), 7.09 (3H, t, $^3J_{HH}$ = 7.5 Hz, Ph), 7.03–6.95 (9H, m, Py/Ph), 6.60 (3H, d, $^3J_{HH}$ = 5.5 Hz, Py), 6.33 (6H, br d, $^3J_{HH}$ = 7.0 Hz, Ph), 5.70 (3H, d, $^2J_{HH}$ = 14.5 Hz, NCH_2Ph), 5.63 (3H, d, $^2J_{HH}$ = 14.5 Hz, NCH_2Ph), 5.32 (3H, dd, $^3J_{HH}$ = 11.0 Hz, 3.0 Hz, CH), 4.70 (3H, d, $^2J_{HH}$ = 11.0 Hz, OCH_2–triazole), 4.46 (3H, d, $^2J_{HH}$ = 11.0 Hz, OCH_2–triazole), 3.59 (3H, t, $^2J_{HH}$/$^3J_{HH}$ = 11.0 Hz, CH_2CHPh), 1.43 (3H, br d, $^2J_{HH}$ = 10.0 Hz, CH_2CHPh).

^{13}C{^{1}H} NMR (100 MHz, 298 K, CD_3CN) δ_C 171.6 (C═N), 159.4, 154.1, 145.8, 142.4, 139.0, 135.0, 130.8, 130.1, 129.9, 129.0, 128.2, 127.8, 126.5, 126.3, 124.8 (Ar, triazole), 72.4 (CHCH_2), 71.1 (CH), 63.4 (OCH_2–triazole), 54.4 (NCH_2Ph–NO_2).

MS (ESI) *m*/*z* 691.23 $[Fe\mathbf{L}^6{}_3]^{2+}$.

Elemental Analysis found (calculated for $C_{72}H_{66}Cl_2CuFeIN_{18}O_{17}$) % C 49.23 (48.79), H 3.84 (3.75), N 14.01 (14.22).

fac,Λ_{Fe},R_C-$[FeL^7{}_3](ClO_4)_2\cdot 3H_2O$

(*R*)-(+)-α-Methylbenzylamine (0.30 ml, 2.33 mmol) was dissolved in acetonitrile (10 ml). 5-(2-Pyridinyloxy)picolinaldehyde (0.5 g, 2.33 mmol) was added, followed by iron(II) perchlorate hexahydrate (0.282 g, 0.78 mmol) to give an immediate colour change to dark pink/purple. After stirring at ambient temperature for 16 h, addition of ethyl acetate (10 ml) caused precipitation of a dark purple powder (0.667 g, 0.55 mmol, 70%) that contained water of crystallisation according to IR spectroscopy. Single crystals were grown by layering a solution in acetonitrile onto ethyl acetate.

^{1}H-NMR (300 MHz, 298 K, CD_3CN): δ 8.51 (bs, 6H, CHN, Py), 7.78 (t, 3H, $^3J_{HH}$ = 7.68 Hz, Py/Ph), 7.25–7.41 (m, 12H, Py/Ph), 7.05 (t, 3H $^3J_{HH}$ = 7.13 Hz, Py/Ph), 6.92 (t, 3H, $^3J_{HH}$ = 7.68 Hz, Py/Ph), 6.51 (d, 3H, $^3J_{HH}$ = 7.68 Hz, Py/Ph), 6.35 (d, 3H, $^3J_{HH}$ = 1.83 Hz, Py/Ph), 5.05–5.20 (m, 9H, PhC$H$$CH_3$, CH_2), 1.87 (d, 9H, $^3J_{HH}$ = 6.46, CH_3).

^{13}C NMR (75 MHz, CD_3CN) δ 170.3 (CHN), 157.9, 155.7, 152.5, 150.5, 143.0, 141.1, 138.2, 130.8, 130.0, 128.3, 125.4, 124.6, 124.5, 123.2, 72.2 (CH_2), 69.3 (*C*HPh).

ESI-MS: 345 $[ML_2]^{2+}$, 503 $[ML_3]^{2+}$, 789 $[ML_2\cdot ClO_4]^+$.

Elemental Analysis found (calculated for $C_{60}H_{63}Cl_2FeN_9O_{14}$) % C 57.16 (57.15), H 4.58 (5.04), N 9.79 (10.00).

fac,Δ_{Fe},S_C-$[FeL^9{}_3](ClO_4)_2$

5-(Propargyloxy)picolinaldehyde (0.50 g, 3.1 mmol) and (*S*)-α-methylbenzylamine (0.38 g, 3.1 mmol) were dissolved in acetonitrile (15 ml) to form a yellow solution. Iron(II) perchlorate hexahydrate (0.38 g, 1.0 mmol, 1.0 eq.) in acetonitrile (5 ml) was added to give a purple solution. This was stirred overnight at ambient temperature before the solvent was removed under reduced pressure. The product, $[Fe\mathbf{L}^9{}_3](ClO_4)_2$, was recrystallised from acetonitrile and ethyl acetate and the resulting purple crystals were filtered and dried *in vacuo*. Yield = 0.65 g, 0.59 mmol, 59%.

^{1}H NMR (400 MHz, 298 K, CD_3CN) δ_H 8.62 (3H, s, HC═N), 7.42–7.35 (6H, m, Py), 7.09 (3H, t, $^3J_{HH}$ = 7.5 Hz, Ph *para*), 7.00 (6H, t, $^3J_{HH}$ = 7.5 Hz, Ph *meta*), 6.62 (6H, d, $^3J_{HH}$ = 7.5 Hz, Ph *ortho*), 6.35 (3H, d, $^4J_{HH}$ = 2.5 Hz, Py), 5.22 (3H, q, $^3J_{HH}$ = 6.5 Hz, CH), 4.72 (3H, dd, $^2J_{HH}$ = 16.5 Hz, $^4J_{HH}$ = 2.5 Hz, CH_2–C═C), 4.64 (3H, dd, $^2J_{HH}$ = 16.5 Hz, $^4J_{HH}$ = 2.5 Hz, CH_2–C═C), 2.94 (3H, t, $^4J_{HH}$ = 2.5 Hz, C═CH), 1.92 (9H, d, $^3J_{HH}$ = 6.5 Hz, CH_3).

^{13}C{^{1}H} NMR (100 MHz, 298 K, CD_3CN) δ_C 170.5 (C═N), 156.7, 152.9, 142.9, 140.9, 130.9, 130.0, 128.4, 125.5, 124.5 (Ar), 79.0 (*C*═CH), 77.7 (C═*C*H), 69.4 (CH), 57.3 (CH_2), 26.3 (CH_3).

MS (ESI) *m*/*z* 424.2 $[Fe\mathbf{L}^9{}_3]^{2+}$.

IR ν cm^{-1} 3256 w, 1592 w, 1560 m, 1496 m, 1452 w, 1383 w, 1297 w, 1278 m, 1229 m, 1070 s, 1007 s, 928 m, 838 m, 760 m, 740 w, 700 s.

Elemental Analysis found (calculated for $C_{51}H_{48}Cl_2FeN_6O_{11}$) % C 58.61 (58.47), H 4.52 (4.62), N 7.94 (8.02).

Notes and references

1 M. Albrecht and R. Fröhlich, *J. Am. Chem. Soc.*, 1997, **119**, 1656–1661.
2 M. Cantuel, G. Bernardinelli, G. Muller, J. P. Riehl and C. Piguet, *Inorg. Chem.*, 2004, **43**, 1840–1849.
3 F. E. Hahn, M. Offermann, C. Schulze Isfort, T. Pape and R. Fröhlich, *Angew. Chem., Int. Ed.*, 2008, **47**, 6794–6797.
4 V. C. M. Smith and J.-M. Lehn, *Chem. Commun.*, 1996, 2733–2734.
5 M. Albrecht, I. Janser, A. Lützen, M. Hapke, R. Fröhlich and P. Weis, *Chem.–Eur. J.*, 2005, **11**, 5742–5748.
6 G. Canard and C. Piguet, *Inorg. Chem.*, 2007, **46**, 3511–3522.
7 N. C. Fletcher, R. T. Brown and A. P. Doherty, *Inorg. Chem.*, 2006, **45**, 6132–6134.
8 S. E. Howson, L. E. N. Allan, N. P. Chmel, G. J. Clarkson, R. van Gorkum and P. Scott, *Chem. Commun.*, 2009, 1727–1729.
9 S. E. Howson, L. E. N. Allan, N. P. Chmel, G. J. Clarkson, R. J. Deeth, A. D. Faulkner, D. H. Simpson and P. Scott, *Dalton Trans.*, 2011, **40**, 10416–10433.
10 S. E. Howson, A. Bolhuis, V. Brabec, G. J. Clarkson, J. Malina, A. Rodger and P. Scott, *Nat. Chem.*, 2012, **4**, 31–36.
11 N. Ousaka, J. K. Clegg and J. R. Nitschke, *Angew. Chem., Int. Ed.*, 2012, **51**, 1464–1468.
12 N. Ousaka, S. Grunder, A. M. Castilla, A. C. Whalley, J. F. Stoddart and J. R. Nitschke, *J. Am. Chem. Soc.*, 2012, **134**, 15528–15537.
13 C. P. Sebli, S. E. Howson, G. J. Clarkson and P. Scott, *Dalton Trans.*, 2010, **39**, 4447–4454.
14 E. J. B. A. Baerends, C. Bo, P. M. Boerrigter, L. Cavallo, L. Deng, R. M. Dickson, D. E. Ellis, L. Fan, T. H. Fischer, C. Fonseca Guerra, S. J. A. van Gisbergen, J. A. Groeneveld, O. V. Gritsenko, F. E. Harris, P. van den Hoek, H. Jacobsen, G. van Kessel, F. Kootstra, E. van Lenthe, V. P. Osinga, P. H. T. Philipsen, D. Post, C. C. Pye, W. Ravenek, P. Ros, P. R. T. Schipper, G. Schreckenbach, J. G. Snijders, M. Sola,

 This journal is © The Royal Society of Chemistry 2013

Open Access Article. Published on 01 August 2013. Downloaded on 10/17/2025 10:08:07 PM.
This article is licensed under a Creative Commons Attribution 3.0 Unported Licence.

D. Swerhone, G. te Velde, P. Vernooijs, L. Versluis, O. Visser, E. van Wezenbeek, G. Wiesenekker, S. K. Wolff, T. K. Woo and T. Ziegler, *adf2008.01*, Scientific Computing and Modelling NV: Free University, Amsterdam, 2008.
15 J. C. Dyason, P. C. Healy, C. Pakawatchai, V. A. Patrick and A. H. White, *Inorg. Chem.*, 1985, **24**, 1957–1960.
16 G. Wilkinson, R. D. Gillard and J. A. McCleverty, in *Comprehensive Coordination Chemistry Volume 5 – Late Transition Elements*, Pergamon Press, Oxford, 1987, pp. 538–551.
17 P. Mobian, J. P. Collin and J. P. Sauvage, *Tetrahedron Lett.*, 2006, **47**, 4907–4909.
18 I. Aprahamian, O. S. Miljanic, W. R. Dichtel, K. Isoda, T. Yasuda, T. Kato and J. F. Stoddart, *Bull. Chem. Soc. Jpn.*, 2007, **80**, 1856–1869.
19 A. I. Prikhod'ko, F. Durola and J.-P. Sauvage, *J. Am. Chem. Soc.*, 2007, **130**, 448–449.
20 S. Durot, P. Mobian, J. P. Collin and J. P. Sauvage, *Tetrahedron*, 2008, **64**, 8496–8503.
21 J. D. Megiatto and D. I. Schuster, *J. Am. Chem. Soc.*, 2008, **130**, 12872–12873.
22 J.-P. Collin, J. Frey, V. r. Heitz, J.-P. Sauvage, C. Tock and L. Allouche, *J. Am. Chem. Soc.*, 2009, **131**, 5609–5620.
23 J.-P. Collin, J.-P. Sauvage, Y. Trolez and K. Rissanen, *New J. Chem.*, 2009, **33**, 2148–2154.
24 J. D. Megiatto and D. I. Schuster, *Chem.–Eur. J.*, 2009, **15**, 5444–5448.
25 A. I. Prikhod'ko and J.-P. Sauvage, *J. Am. Chem. Soc.*, 2009, **131**, 6794–6807.
26 J. P. Collman, N. K. Devaraj and C. E. D. Chidsey, *Langmuir*, 2004, **20**, 1051–1053.
27 S.-i. Fukuzawa, H. Oki, M. Hosaka, J. Sugasawa and S. Kikuchi, *Org. Lett.*, 2007, **9**, 5557–5560.
28 D. Gonzalez Cabrera, B. D. Koivisto and D. A. Leigh, *Chem. Commun.*, 2007, 4218–4220.
29 C. Haensch, M. Chiper, C. Ulbricht, A. Winter, S. Hoeppener and U. S. Schubert, *Langmuir*, 2008, **24**, 12981–12985.
30 M. Jauregui, W. S. Perry, C. Allain, L. R. Vidler, M. C. Willis, A. M. Kenwright, J. S. Snaith, G. J. Stasiuk, M. P. Lowe and S. Faulkner, *Dalton Trans.*, 2009, 6283–6285.
31 A. R. McDonald, H. P. Dijkstra, B. M. J. M. Suijkerbuijk, G. P. M. van Klink and G. van Koten, *Organometallics*, 2009, **28**, 4689–4699.
32 E. C. Constable, C. E. Housecroft, M. Neuburger and P. Rosel, *Chem. Commun.*, 2010, **46**, 1628–1630.
33 S. E. Howson and P. Scott, *Dalton Trans.*, 2011, **40**, 10268–10277.
34 S. Paliwal, S. Geib and C. S. Wilcox, *J. Am. Chem. Soc.*, 1994, **116**, 4497–4498.
35 M. Nishio, *CrystEngComm*, 2004, **6**, 130–158.
36 J. L. M. Abboud, C. Foces-Foces, R. Notario, R. E. Trifonov, A. P. Volovodenko, V. A. Ostrovskii, I. Alkorta and J. Elguero, *Eur. J. Org. Chem.*, 2001, 3013–3024.
37 L. Zhang, X. Chen, P. Xue, H. H. Y. Sun, I. D. Williams, K. B. Sharpless, V. V. Fokin and G. Jia, *J. Am. Chem. Soc.*, 2005, **127**, 15998–15999.
38 B. C. Boren, S. Narayan, L. K. Rasmussen, L. Zhang, H. Zhao, Z. Lin, G. Jia and V. V. Fokin, *J. Am. Chem. Soc.*, 2008, **130**, 8923–8930.
39 J. R. Johansson, P. Lincoln, B. Nordén and N. Kann, *J. Org. Chem.*, 2011, **76**, 2355–2359.
40 C. N. Urbani, C. A. Bell, M. R. Whittaker and M. J. Monteiro, *Macromolecules*, 2008, **41**, 1057–1060.
41 C. Ornelas, J. Broichhagen and M. Weck, *J. Am. Chem. Soc.*, 2010, **132**, 3923–3931.
42 S. E. Howson, L. E. N. Allan, N. P. Chmel, G. J. Clarkson, R. van Gorkum and P. Scott, *Chem. Commun.*, 2009, 1727–1729.
43 M. Seredyuk, A. B. Gaspar, V. Ksenofontov, Y. Galyametdinov, J. Kusz and P. Gütlich, *J. Am. Chem. Soc.*, 2008, **130**, 1431–1439.
44 H. C. Kolb, M. G. Finn and K. B. Sharpless, *Angew. Chem., Int. Ed.*, 2001, **40**, 2004–2021.
45 S. J. Coles and P. A. Gale, *Chem. Sci.*, 2012, **3**, 683–689.
46 G. M. Sheldrick, *Acta Crystallogr., Sect. A: Fundam. Crystallogr.*, 2008, **64**, 112–122.
47 S. Grimme, *J. Comput. Chem.*, 2004, **25**, 1463–1473.
48 E. J. Baerends, D. E. Ellis and P. Ros, *Theor. Chim. Acta*, 1972, **27**, 339–354.
49 C. C. Pye and T. Ziegler, *Theor. Chem. Acc.*, 1999, **101**, 396–408.
50 R. L. Bixler and C. Niemann, *J. Org. Chem.*, 1958, **23**, 575–584.
51 E. J. O'Neil, K. M. DiVittorio and B. D. Smith, *Org. Lett.*, 2007, **9**, 199–202.